
Multi-Agent Conformal Prediction with Personalized Statistical Validity

Martin V. Vejling

Department of Electronic Systems
Aalborg University, Aalborg, Denmark
mvv@es.aau.dk

Christophe A. N. Biscio

Department of Mathematical Sciences
Aalborg University, Aalborg, Denmark
christophe@math.aau.dk

Adrien Mazoyer

Institut de Mathématiques de Toulouse
Université de Toulouse, Toulouse, France
adrien.mazoyer@math.univ-toulouse.fr

Petar Popovski

Department of Electronic Systems
Aalborg University, Aalborg, Denmark
petarp@es.aau.dk

Shashi Raj Pandey

Department of Electronic Systems
Aalborg University, Aalborg, Denmark
srp@es.aau.dk

Abstract

Uncertainty quantification is essential in high-stakes machine learning tasks. However, one of the principled solutions, *conformal prediction*, faces challenges under limited local calibration data, privacy constraints, and data heterogeneity. In multi-agent settings, existing works do not simultaneously and satisfactorily address these challenges with guarantees either limited to averages across agents or losing validity in heterogeneous settings. Hence, we propose **personalized federated weighted conformal prediction (PFWCP)**, a framework that combines local density ratio weighting with weighted quantile aggregation to correct for heterogeneity while preserving privacy. The method yields asymptotically valid marginal and calibration-conditional coverage guarantees for each participating agent and supports protocols with one-shot communication. Theoretical analysis presents an adjustment to the coverage variance, governed by an effective sample size expression, which is necessary in the context of weighted conformal prediction, and experiments on synthetic and real datasets show improved calibration quality over state-of-the-art federated conformal baselines.

1 Introduction

Uncertainty quantification (UQ) is a key component of modern machine learning systems, especially in high-stakes settings where decisions must be accompanied by measures of reliability (Campagner et al. 2025). Conformal prediction (CP) offers rigorous, distribution-free statistical guarantees with improved quality, in terms of tighter prediction sets and more stable coverage behavior, as the amount of quality calibration data increases (Vovk et al. 2005).

In many realistic applications, a single organization or agent may only have access to a limited amount of local data (Rieke et al. 2020). This makes it difficult to obtain both valid and efficient guarantees using CP in isolation. A possible remedy is to pool data from multiple data agents (DAs), however, in such collaborative settings, the data distributions are often heterogeneous across agents,

which can lead to systematic violations of the exchangeability assumptions underpinning standard CP (Lu et al. 2023). A principled multi-agent conformal method must account for heterogeneity in how it weights and aggregates calibration information from each agent while being privacy-aware.

Existing federated conformal prediction (FCP) approaches only partially address this challenge: some methods maintain privacy and support one-shot communication but assume homogeneous data, leading to severe miscoverage under covariate shift (Humbert et al. 2023, 2024), while others do not provide personalized coverage guarantees (Lu et al. 2023, Srinivasan et al. 2025, Wen et al. 2026). Some use weighted conformal prediction (WCP) to correct coverage bias but fail to correctly adjust for the shift in coverage variance, require multiple communication rounds, and typically provide only marginal coverage (MC), not calibration-conditional coverage (CCC), guarantees (Plassier et al. 2023, 2024). As a result, none of them simultaneously delivers per-agent coverage guarantees, data privacy, robustness to heterogeneity, and communication efficiency.

This paper introduces a personalized federated weighted conformal prediction (PFWCP) framework that jointly corrects for bias and variance induced by data heterogeneity while preserving privacy and requiring only lightweight communication. The key idea is to combine density-ratio-based weighting of conformal scores at each agent with a weighted-quantile-of-quantiles aggregation at the server, calibrated through an approximation of the per agent CCC distribution. This yields prediction sets that (i) provide asymptotically valid MC and CCC guarantees for each participating agent under covariate shift between agents, and (ii) can be implemented in both standard and one-shot federated protocols with minimal additional overhead.

Problem formulation: We have an interest in both MC and CCC guarantees. In the first, for a given significance level α , FCP constructs a prediction set, denoted \mathcal{C}_α , which for a given test covariate X returns a set-valued prediction with guarantee on the MC, i.e.,

$$\mathbb{P}(Y \in \mathcal{C}_\alpha(X)) \geq 1 - \alpha,$$

where Y denotes the true label. Implicitly, the prediction set depends on calibration data which in the case of FCP is distributed among the participating DAs. In the second, for given significance levels α and δ , FCP constructs a prediction set, denoted $\mathcal{C}_{\alpha,\delta}$, providing a guarantee on the CCC, i.e.,

$$\mathbb{P}_{\mathcal{D}}(\mathbb{P}(Y \in \mathcal{C}_{\alpha,\delta}(X)|\mathcal{D}) \geq 1 - \alpha) \geq 1 - \delta,$$

where we use \mathcal{D} to denote the calibration data following distribution $\mathbb{P}_{\mathcal{D}}$. The purpose of this work is to design prediction sets $\mathcal{C}_\alpha(X)$ (or $\mathcal{C}_{\alpha,\delta}(X)$) in a federated setting while being efficient, i.e., minimizing the expected size of the prediction sets, while satisfying the statistical guarantees presented above.

Similarly to Min et al. (2025), we consider a federated learning (FL) scenario with K DAs. The k -th DA, for $k \in [K] = \{1, \dots, K\}$, observes \tilde{n}_k training data points $\tilde{\mathcal{D}}^k = \{\tilde{Z}_i^k\}_{i=1}^{\tilde{n}_k}$, $\tilde{Z}_i^k = (\tilde{X}_i^k, \tilde{Y}_i^k)$, from unknown distribution $\mathbb{P}^k = \mathbb{P}_{Y|X} \mathbb{P}_X^k$ on the sample space $\mathcal{Z} = \mathcal{X} \times \mathcal{Y}$, and n_k exchangeable calibration data points $\mathcal{D}^k = \{Z_i^k\}_{i=1}^{n_k}$, $Z_i^k = (X_i^k, Y_i^k)$, from the same distribution \mathbb{P}^k . We denote by $\mathcal{D} = \bigcup_{k=1}^K \mathcal{D}^k$ the total calibration data, although this data is at no point centralized. For a test point $Z = (X, Y) \sim \mathbb{P} = \mathbb{P}_{Y|X} \mathbb{P}_X$ of unknown test distribution \mathbb{P} where only X is observed, the objective is to provide a prediction set for Y satisfying either MC or CCC guarantees.

We make the following general assumptions: (A1) for each k , $Z_1^k, \dots, Z_{n_k}^k$ are exchangeable; (A2) the data in \mathcal{D}^k is independent of the data in \mathcal{D}^l for $k \neq l$; and (A3) the data in $\tilde{\mathcal{D}} = \bigcup_{k=1}^K \tilde{\mathcal{D}}^k$ is independent of the data in \mathcal{D} . We consider a practical scenario where the data is heterogeneous due to a covariate shift, i.e., $\mathbb{P}_X^k \neq \mathbb{P}_X^l$ for $k \neq l$, and, in line with Min et al. (2025), without loss of generality, the test data is observed by DA 1, hence, $\mathbb{P} = \mathbb{P}^1$. In this sense, the objective is personalization: we strive for a valid and efficient conformal predictor for each individual DA under data heterogeneity.

Preview of proposed method: With the training data, $\tilde{\mathcal{D}}$, a prediction model is trained, in turn defining a non-conformity score function $\hat{s} : \mathcal{Z} \rightarrow \mathbb{R}$, which is evaluated on the calibration data, $\hat{s}_i^k = \hat{s}(X_i^k, Y_i^k)$. In line with WCP, as introduced by Tibshirani et al. (2019), weight functions $\hat{\omega}^k : \mathcal{X} \rightarrow \mathbb{R}$ are defined as estimators of the density ratios $\omega^k(X) = [d\mathbb{P}_X / d\mathbb{P}_X^k](X)$ which for $k \in \{2, \dots, K\}$ are fitted using the training data, while $\hat{\omega}^1 \equiv 1$, and then evaluated on the calibration

Table 1: Comparison with closest related works. Shorthands: Federated calibration (Fed. cali.); Privacy-preserving (Priv.-pres.); Heterogeneous (Het.); Personalized (Pers.); adjusted (adj.).

	Fed. cali.	One-shot	CCC	Priv.-pres.	Het.	Pers.	Bias adj.	Var adj.
Lu et al. (2023)	✓	✗	✗	✓	✓	✗	N/A	N/A
Plassier et al. (2023, 2024)	✓	✗	✗	✓	✓	✓	✓	✗
Humbert et al. (2023, 2024)	✓	✓	✓	✓	✗	✗	N/A	N/A
Min et al. (2025)	✗	✓	✓	✓	✓	✓	N/A	N/A
Ours	✓	✓	✓	✓	✓	✓	✓	✓

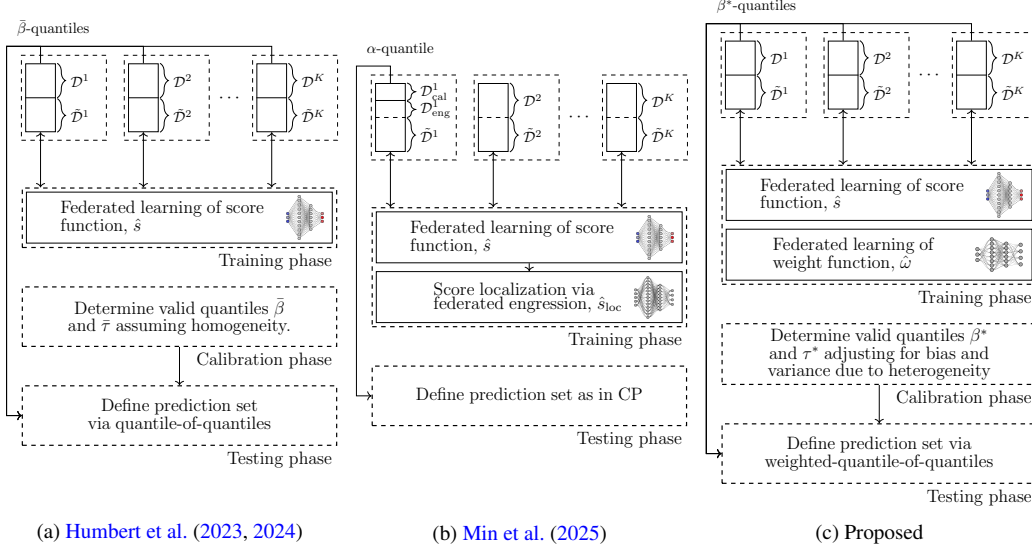


Figure 1: Outline of the proposed methodology with comparison to the closest existing works.

data, $\hat{\omega}_i^k = \hat{\omega}(X_i^k)$. We propose to use a weighted-quantile-of-quantiles method, constructing the prediction set as $\mathcal{C}_{\beta, \tau}^{\text{wqq}}(X) = \{Y \in \mathcal{Y} : \hat{s}(X, Y) \leq Q_{\beta, \tau}\}$ for

$$Q_{\beta, \tau} = \text{Quantile}\left(1 - \tau; \sum_{k=1}^K w_k \delta_{Q_{\beta}^k}\right), \text{ where } Q_{\beta}^k = \text{Quantile}\left(1 - \beta; \frac{\sum_{i=1}^{n_k} \hat{\omega}_i^k \delta_{\hat{s}_i^k} + \hat{\omega}^k(X) \delta_{\infty}}{\bar{\omega}^k + \hat{\omega}^k(X)}\right),$$

where $\bar{\omega}^k = \sum_{j=1}^{n_k} \hat{\omega}_j^k$ is the total calibration data weight, β and τ are the local and aggregation quantiles, respectively, and w_k are normalized weights used to emphasize contributions from DAs with higher data distribution similarity. To provide statistically valid prediction sets, quantiles β^* and τ^* should be determined such that $\mathcal{C}_{\beta^*, \tau^*}^{\text{wqq}}(X)$ satisfies either MC or CCC guarantees. To enable this, we show in this paper that, as $n_1, \dots, n_K \rightarrow \infty$,

$$\mathbb{P}(Y \in \mathcal{C}_{\beta, \tau}^{\text{wqq}}(X) | \mathcal{D}) \xrightarrow{d} \text{Quantile}\left(1 - \tau; \sum_{k=1}^K w_k \delta_{U_{\beta}^k}\right),$$

where $U_{\beta}^k \sim \text{Beta}((1 - \beta)(n_{\text{eff}}^k + 1), \beta(n_{\text{eff}}^k + 1))$ for $n_{\text{eff}}^k = \|\hat{\omega}_1^k, \dots, \hat{\omega}_{n_k}^k\|_1^2 / \|\hat{\omega}_1^k, \dots, \hat{\omega}_{n_k}^k\|_2^2$ which are referred to as the local effective sample sizes.

Related works: Lu et al. (2023) introduced a notion of partial exchangeability leading to statistically valid FCP if the test distribution is a mixture of the calibration distributions and addressed privacy of score distribution via sketching. This was extended to conformal fairness by Srinivasan et al. (2025) and to group-conditional guarantees in Wen et al. (2026). Meanwhile, using the idea of WCP originally proposed by Tibshirani et al. (2019), Plassier et al. (2023) developed FCP under label shift, followed by a study for the case of covariate shift in Plassier et al. (2024) which is able to correct the coverage bias induced by the covariate shift at the cost of an increased variance. Their approach requires multiple rounds of communication for quantile estimation and provides no CCC guarantees. In another work, Li et al. (2026) study federated conformal prediction under label shift

and propose a score function building on the idea of adaptive prediction sets including also a local and global prototype similarity score.

A different FCP method was proposed in [Humbert et al. \(2023, 2024\)](#) based on the idea of sharing only a quantile of the scores and then at the central agent taking the quantile-of-quantiles, providing a privacy-preserving solution requiring just one-shot communication, contrary to FCP mentioned above. While effective for homogeneous data scenarios, severe issues arise under data heterogeneity. The proposed weighted-quantile-of-quantiles method can be viewed as a generalization of the quantile-of-quantiles approach that is designed to deal with data heterogeneity, and the quantile-of-quantiles is the particularly special case when the density ratios are constantly one, $\hat{\omega}^k(X) \equiv 1$.

The idea of quantile-of-quantiles is closely related to the majority voting scheme of [Cherubin \(2019\)](#) which notably studies two methods: (i) the overly conservative C-method which bounds the coverage using the Markov inequality, and (ii) the overly liberal I-method that assumes independence of the events $\hat{s}(X, Y) \leq Q_\beta^k$. With this perspective, this work proposes an intermediate solution between the overly conservative C-method and overly liberal I-method.

Recently, [Min et al. \(2025\)](#) proposed to use decentralized data for localizing the score function employing federated engrression and relying only on local data for calibration. This avoids the challenging issue with non-exchangeability in CP, however, the efficiency is restricted by the availability of local data.

A comparison of the present work with the existing literature is given in Table 1. Note that our method aim at solving all the limitations aforementioned. We are using calibration data from all agents (Fed. cali.), preserve privacy (Priv.-pres), require only one-shot communication round (One-shot) and provide MC and CCC guarantees valid for each individual agent (Pers.) under data heterogeneity (Het.) with appropriate adjustments to account for bias and variance induced by the data heterogeneity. To better see the differences between our approach and the ones proposed by [Humbert et al. \(2023, 2024\)](#) and [Min et al. \(2025\)](#), we have outlined them in Figure 1.

2 Personalized federated weighted conformal prediction

We now give a detailed description of the proposed PFWCP framework. We divide the framework into three phases: (i) the training phase where the training data $\tilde{\mathcal{D}}$ is used to learn the score and weight functions using federated algorithms; (ii) the calibration phase where scores and weights are evaluated on the calibration data \mathcal{D} ; and (iii) the testing phase where given a test covariate X the conformal prediction set $\mathcal{C}_\alpha(X)$ (or $\mathcal{C}_{\alpha,\delta}(X)$) is constructed.

Training phase: we begin by training a prediction model $\hat{f} : \mathcal{X} \rightarrow \mathcal{Y}$ on $\tilde{\mathcal{D}}$ using federated learning and define from this a non-conformity score function $\hat{s} : \mathcal{X} \times \mathcal{Y} \rightarrow \mathbb{R}$. Weight functions, defined as estimators of the density ratios $[\text{d}\mathbb{P}_X/\text{d}\mathbb{P}_X^k](X)$ for $k \in \{2, \dots, K\}$, are trained on $\tilde{\mathcal{D}}$ using federated learning and denoted $\hat{\omega}^k$, and $\hat{\omega}^1(X) \equiv 1$.

Calibration phase: on the calibration data, evaluate the non-conformity scores $\hat{s}_i^k = \hat{s}(X_i^k, Y_i^k)$ and the density ratio weights $\hat{\omega}_i^k = \hat{\omega}^k(X_i^k)$ for $k \in \{2, \dots, K\}$ and $i \in [n_k]$, and compute local effective sample sizes $n_{\text{eff}}^k = \|\hat{\omega}_1^k, \dots, \hat{\omega}_{n_k}^k\|_1^2 / \|\hat{\omega}_1^k, \dots, \hat{\omega}_{n_k}^k\|_2^2$, and normalized distribution similarity weights w_k for $k \in \{2, \dots, K\}$. For a local quantile $\beta \in (0, 1)$ and an aggregate quantile $\tau \in [0, 1]$, the prediction set is $\mathcal{C}_{\beta,\tau}^{\text{wqq}}(X) = \{Y \in \mathcal{Y} : \hat{s}(X, Y) \leq Q_{\beta,\tau}\}$ for

$$Q_{\beta,\tau} = \text{Quantile}\left(1 - \tau; \sum_{k=1}^K w_k \delta_{Q_\beta^k}\right), \text{ where } Q_\beta^k = \text{Quantile}\left(1 - \beta; \frac{\sum_{i=1}^{n_k} \hat{\omega}_i^k \delta_{\hat{s}_i^k} + \hat{\omega}^k(X) \delta_\infty}{\bar{\omega}^k + \hat{\omega}^k(X)}\right). \quad (1)$$

The core principle of the proposed methodology is that the CCC for the k -th DA can be approximated by $U_\beta^k \sim \text{Beta}((1 - \beta)(n_{\text{eff}}^k + 1), \beta(n_{\text{eff}}^k + 1))$. Specifically, according to Proposition 1, as $n_1, \dots, n_K \rightarrow \infty$,

$$\mathbb{P}(\hat{s}(X, Y) \leq Q_{\beta,\tau} | \mathcal{D}) = \mathbb{P}(F_{\hat{s}}^{-1}(U) \leq Q_{\beta,\tau} | \mathcal{D}) \xrightarrow{d} U_\beta^{(\tau)}, \quad (2)$$

where $F_{\hat{s}}$ is the cumulative distribution function (CDF) of the non-conformity scores assumed to be continuous, $U \sim \text{Uniform}([0, 1])$, and $U_\beta^{(\tau)} = \text{Quantile}(1 - \tau; \sum_{k=1}^K w_k \delta_{U_\beta^k})$.

Procedure 1 Marginal coverage

- Input: Significance level $\alpha \in (0, 1)$; Effective samples sizes $n_{\text{eff}}^1, \dots, n_{\text{eff}}^K \leq n$; Grid $\mathcal{G} \subset (0, 1) \times [0, 1)$; Monte Carlo repetitions $N_{\text{rep}} \in \mathbb{N}$.
- 1: Compute weights $w_k = n_{\text{eff}}^k / (\sum_{k=1}^K n_{\text{eff}}^k)$ for $k \in [K]$;
 - 2: **for each** $(\beta, \tau) \in \mathcal{G}$ **do**
 - 3: **for each** $i \in \{1, \dots, N_{\text{rep}}\}$ **do**
 - 4: Sample $U_{\beta}^k \sim \text{Beta}((1 - \beta)(n_{\text{eff}}^k + 1), \beta(n_{\text{eff}}^k + 1))$ for $k \in [K]$;
 - 5: $U_{\beta, i}^{(\tau)} \leftarrow \text{Quantile}(1 - \tau; \sum_{k=1}^K w_k \delta_{U_{\beta}^k})$;
 - 6: **end for**
 - 7: $\text{Cov}_{\beta, \tau} \leftarrow \frac{1}{N_{\text{rep}}} \sum_{i=1}^{N_{\text{rep}}} U_{\beta, i}^{(\tau)}$;
 - 8: **end for**
 - 9: Find $(\beta^*, \tau^*) \leftarrow \arg \min_{(\beta, \tau) \in \mathcal{G}} \{\text{Cov}_{\beta, \tau} : \text{Cov}_{\beta, \tau} \geq 1 - \alpha\}$;
- Output: (β^*, τ^*) .
-

For MC, given significance level α , we determine quantile parameters (β^*, τ^*) such that $\mathbb{P}(Y \in \mathcal{C}_{\beta^*, \tau^*}^{\text{wqq}}(X)) \geq 1 - \alpha$ while optimizing the efficiency. This is approximately achieved by minimizing $\mathbb{E}[U_{\beta^*}^{(\tau^*)}]$ under constraint $\mathbb{E}[U_{\beta^*}^{(\tau^*)}] \geq 1 - \alpha$, concretely

$$(\beta^*, \tau^*) = \arg \min_{\beta, \tau} \{ \mathbb{E}[U_{\beta}^{(\tau)}] : \mathbb{E}[U_{\beta}^{(\tau)}] \geq 1 - \alpha \}. \quad (3)$$

This optimization problem does not admit an analytical solution, and in fact, $\mathbb{E}[U_{\beta}^{(\tau)}]$ has no simple expressive formula. Rather, we approximate $\mathbb{E}[U_{\beta}^{(\tau)}]$ using Monte Carlo simulations, as outlined in Procedure 1. We remark here that the choice of the hyperparameter N_{rep} represents an important trade-off between computational complexity and the error made in solving Eq. (3). A discussion regarding setting N_{rep} is provided in Section S3.3.

CCC can be achieved using similar methodology as for MC. The objective is here to determine hyperparameters β_c^* and τ_c^* such that the CCC is minimized while maintaining

$$\mathbb{P}_{\mathcal{D}}(\mathbb{P}(Y \in \mathcal{C}_{\beta_c^*, \tau_c^*}^{\text{wqq}}(X) | \mathcal{D}) \geq 1 - \alpha) \geq 1 - \delta,$$

for given significance levels α and δ . We propose to approximate the left-side of the above inequality by $\mathbb{P}(U_{\beta}^{(\tau)} \geq 1 - \alpha)$ which can be numerically approximated through Monte Carlo simulations. Concretely, we replace line 7 in Procedure 1 by $\text{CCov}_{\beta, \tau} \leftarrow \frac{1}{N_{\text{rep}}} \sum_{i=1}^{N_{\text{rep}}} \mathbb{1}[U_{\beta, i}^{(\tau)} \geq 1 - \alpha]$ and line 9 by $(\beta_c^*, \tau_c^*) \leftarrow \arg \min_{(\beta, \tau) \in \mathcal{G}} \{\text{CCov}_{\beta, \tau} : \text{CCov}_{\beta, \tau} \geq 1 - \delta\}$.

Testing phase: DA 1 shares the test weight $\hat{\omega}(X)$ which in turn enables the computation of the quantiles $Q_{\beta_c^*}^k$ (or $Q_{\beta_c^*}^k$). These quantiles are shared with the central server that computes the weighted-quantile-of-quantiles $Q_{\beta_c^*, \tau_c^*}$ (or $Q_{\beta_c^*, \tau_c^*}$) and shares it with DA 1. Finally, the conformal prediction set is constructed as $\mathcal{C}_{\beta_c^*, \tau_c^*}^{\text{wqq}}(X)$ (or $\mathcal{C}_{\beta_c^*, \tau_c^*}^{\text{wqq}}(X)$).

Remark 1 (Designing the weights). *In line with the technique of Tibshirani et al. (2019), we train $K - 1$ binary classifiers, $\hat{g}_k : \mathcal{X} \rightarrow (0, 1)$, using federated learning with training data $\{(\tilde{X}_i^k, 0)\}_{i=1}^{\tilde{n}_k} \cup \{(\tilde{X}_i^1, 1)\}_{i=1}^{\tilde{n}_1}$. Then, $\hat{\omega}^k(X) = \hat{g}_k(X) / (1 - \hat{g}_k(X))$ where $\hat{g}_k(X)$ denotes the estimated probability that X belongs to class 1 for $k \in \{2, \dots, K\}$. A detailed discussion motivating this construction as well as potential alternatives is presented in Section S2.*

We define aggregation weights $w_k \propto n_{\text{eff}}^k$. This choice of aggregation weights is natural as it imposes no further computation or communication overhead, and n_{eff}^k can be interpreted as a type of distribution similarity measure: a large n_{eff}^k is indicative of a high distribution similarity, and vice versa. A discussion of alternatives is given in Section S2.

One-shot personalized federated weighted conformal prediction (osPFWCP) The PFWCP method requires each participating DA to share a quantile for each arriving test point since the quantiles in WCP changes depending on the test point covariate through the weight $\hat{\omega}^k(X)$. We present

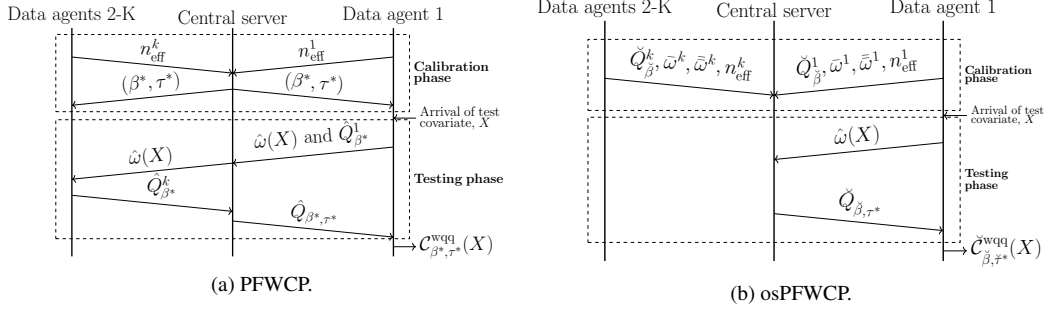


Figure 2: Diagrams illustrating the communication signaling required to execute the PFWCP and osPFWCP algorithms.

now a procedure allowing the participating DAs to share only a single quantile in the calibration phase (prior to testing), and then simply adjust the outer quantile, τ , depending on the arriving test covariate, in order to provide the required statistical guarantees. Thereby, the method requires only minimal communication signaling during the testing phase, however, at the cost of less flexibility in choosing the inner quantile, β .

Fix an inner quantile, $\check{\beta}$, and construct the prediction set as $\check{C}_{\check{\beta}, \tau}^{\text{wqq}}(X) = \{Y \in \mathcal{Y} : \hat{s}(X, Y) \leq \check{Q}_{\check{\beta}, \tau}^k\}$ for

$$\check{Q}_{\check{\beta}, \tau}^k = \text{Quantile}\left(1 - \tau; \sum_{k=1}^K w_k \delta_{\check{Q}_{\check{\beta}}^k}\right), \text{ where } \check{Q}_{\check{\beta}}^k = \text{Quantile}\left(1 - \check{\beta}; \frac{\sum_{i=1}^{n_k} \hat{\omega}_i^k \delta_{\hat{s}_i^k}}{\bar{\omega}^k}\right). \quad (4)$$

By doing this, the quantiles, $\check{Q}_{\check{\beta}}^k$, are computed and shared with the central server only once during the calibration phase, along with added information $\bar{\omega}^k$ and $\bar{\omega}^k = \sum_{i=1}^{n_k} \hat{\omega}_i^k \mathbb{1}[\hat{s}_i^k > \check{Q}_{\check{\beta}}^k]$. At the central server, given the test covariate, X , β^k -quantiles such that $\check{Q}_{\check{\beta}}^k = Q_{\beta^k}^k$ are derived as $\beta^k = (\hat{\omega}^k(X) + \bar{\omega}^k) / (\bar{\omega}^k + \hat{\omega}^k(X))$. Finally, the central server finds a quantile $\check{\tau}^*$ to realize the required statistical guarantee following an algorithm similar to Procedure 1, but limiting the parameter search to the outer quantile parameter, τ , and using the inner quantiles β^1, \dots, β^K . The complexity of this is relatively low since it is only a one-dimensional parameter search.

An overview of the communication signaling required to execute either the PFWCP or one-shot personalized federated weighted conformal prediction (osPFWCP) algorithms is given in Figure 2, illustrating clearly the benefits of the one-shot approach by noticing that minimal communication signaling is required during the testing phase.

Limitations: The scope of the present study is limited to dealing with covariate shifts, and it will be interesting to extend the methodology to more general types of distribution shifts. Further, the presented methodology has some limitations. Namely, since the methods rely on estimating the density ratio, if this is poorly approximated, it will result in failure to properly adjust for the bias and variance in the coverage due to the data heterogeneity. Such a risk is, however, unavoidable when calibrating in the presence of unknown distribution shifts, hence, the limitation is shared with existing works (Plassier et al. 2024). Finally, some care has to be taken in the selection of the β and τ quantiles, mainly, it is crucial that $\sum_{i=1}^{n_k} \hat{\omega}_i^k \geq (1 - \beta)(\bar{\omega}^k + \hat{\omega}^k(X))$ for all $k \in [K]$, otherwise Q_{β}^k will not be finite. This can be dealt with by limiting the search space over β and τ to moderate values, see also the discussion in Section S3.3.

Key theoretical result: The key result motivating the proposed methodology is now rigorously presented. The proof is inspired by Gretton et al. (2009) and is presented in detail in Section S1.

Proposition 1. Assume that the score function is continuously distributed, that $\hat{\omega}^k \equiv \omega^k$, that \mathbb{P} is absolutely continuous with respect to \mathbb{P}^k for $k \in [K]$, and that there exists bounded constants $0 < A \leq 1 \leq B$ such that $\mathbb{P}_X^k(\omega(X_i^k) \in [A, B]) = 1$ for $X_i^k \sim \mathbb{P}_X^k$, $k \in [K]$, $i \in [n_k]$. Then, as

$n_1, \dots, n_K \rightarrow \infty$,

$$\mathbb{P}(Y \in \mathcal{C}_{\beta, \tau}^{\text{wqq}}(X) | \mathcal{D}) \stackrel{d}{\rightarrow} \text{Quantile}\left(1 - \tau; \sum_{k=1}^K w_k \delta_{U_{\beta}^k}\right),$$

where $U_{\beta}^k \sim \text{Beta}((1 - \beta)(n_{\text{eff}}^k + 1), \beta(n_{\text{eff}}^k + 1))$ for $n_{\text{eff}}^k = \|\omega_1^k, \dots, \omega_{n_k}^k\|_1^2 / \|\omega_1^k, \dots, \omega_{n_k}^k\|_2^2$.

This result directly supports the core argument from Eq. (2), thereby providing the theoretical justification for Procedure 1. Notably, the approximation of Eq. (2) relies on accurate estimation of the density ratios and a sufficiently large calibration data size: as the proof indicates, the error of the approximation decays as the calibration data sizes increase. The result is complementary to that of Pournaderi & Xiang (2026) which also dealt with CCC of WCP considering the problem through concentration inequalities. Applying their result is, however, not practically straightforward in our setting due to the presence of unknown constants in the expressed CCC bounds.

We conducted a numerical experiment on the Tennessee’s student teacher achievement ratio dataset (Achilles et al. 2008), simulating data heterogeneity with exponential tilting as in Tibshirani et al. (2019) (details on the data setup are found in Section S3.4). The result is shown in Figure 3.

The quantile-of-quantiles method of Humbert et al. (2023, 2024) approximates the solid blue line with the dashed red line resulting in severe miscoverage. On the other hand, Plassier et al. (2023, 2024) approximates the solid purple line with the dashed red line, while we propose to approximate it with the dashed purple line. Figure 3 clearly illustrates the benefits of the proposed approximation as compared to the alternatives from the literature.

3 Numerical experiments

In this section, we report results from numerical experiments that study the performance in terms of miscoverage and efficiency of the proposed conformal predictors with those of relevant benchmarks.

The experiments cover nine datasets: two synthetic regression datasets (*Gaussian* and *Poisson*), six real regression datasets (*airfoil*, *bike*, *concrete*, *crime*, *star*, and *protein*) also considered in Tibshirani et al. (2019), Humbert et al. (2023, 2024), Min et al. (2025), and a real classification dataset (*cifar10c*). Details regarding the datasets and how data heterogeneity is generated are found in Section S3.1. The prediction model is defined as a fully connected neural network, and likewise for the density ratio estimators. The predictors and density ratio estimators are trained in a federated learning setting and each of the $K = 11$ DAs has $\tilde{n}_k = 50$ training data points. For calibration, each DA has $n_k = 100$ additional data points. Details of model specifications and training are found in Section S3.3. For the regression tasks, we use as non-conformity score $\hat{s}(X, Y) = |Y - \hat{f}(X)|$ where \hat{f} is the trained regression model, while for the classification task, we use $\hat{s}(X, Y) = 1 - [\hat{f}(X)]_Y$ where $[\hat{f}(X)]_Y$ denotes the softmax output of the trained classifier \hat{f} associated with the label Y .

As benchmarks we include vanilla CP (*CP*), federated generalized localization conformal prediction as in Min et al. (2025) (*FGLCP*), quantile-of-quantiles as in Humbert et al. (2023, 2024) (*FCP-QQ*), and federated WCP Plassier et al. (2024) (*FWCP*). Variants of our proposal are included, herein, federated WCP by quantile-of-quantiles (*FWCP-QQ*), personalized federated WCP (*PFWCP*), one-shot personalized federated WCP (*osPFWCP*), and one-shot personalized federated WCP with federated generalized localization (*osPFWGLCP*). Details of benchmarks are given in Section S3.2. As performance metrics, for a conformal predictor denoted \mathcal{C} , we use the MC and CCC when relevant, and further express the conditional miscoverage (CMC), defined as $\mathbb{E}[\mathbb{P}(Y \in \mathcal{C} | \mathcal{D}) - (1 - \alpha)]$, and the efficiency (Eff.), defined as $\mathbb{E}[|\mathcal{C}|]$. These quantities are estimated through Monte Carlo simulations covering 500 calibration data simulations with 500 test data points for each.

Marginal coverage: We display in Figure 4, boxplots of the coverage and efficiency with all the benchmark methodologies providing MC guarantees, on the *star* dataset, when setting the significance level to $\alpha = 0.1$. This result shows the high variability in coverage and prediction set size of *CP* and *FGLCP* due to only using local data for calibration, and also highlights the miscoverage with the *FCP-QQ* and *FWCP-QQ* methods due to failure to correct for the bias and variance shifts in the coverage caused by the data heterogeneity. Meanwhile, the proposed methods has only

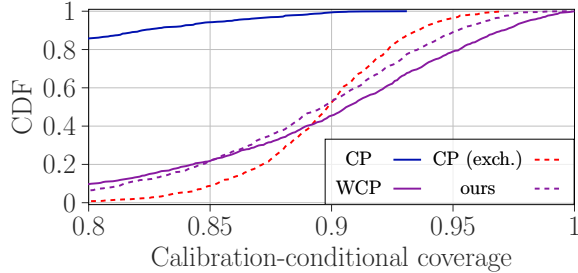


Figure 3: Empirical CDF of the CCC for CP with covariate shift (blue solid line), CP without covariate shift (red dashed line), WCP (purple solid line), and CP without covariate shift but samples limited to the effective sample size (purple dashed line). Significance level $\alpha = 0.1$ and calibration data size $n = 100$.

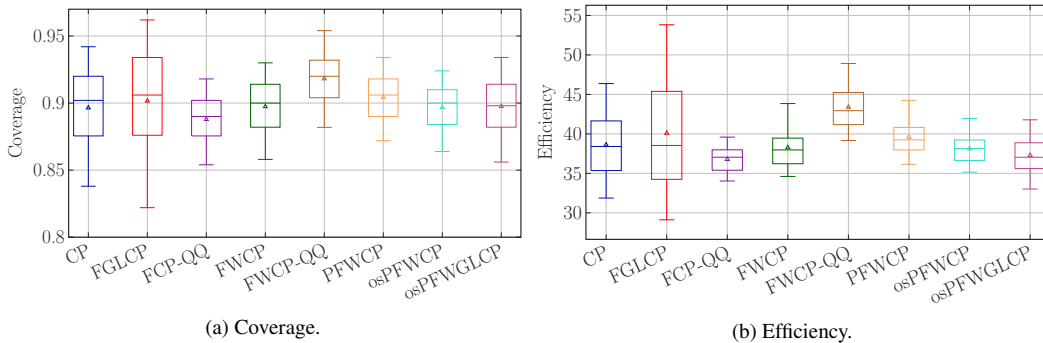


Figure 4: Boxplots of coverage and efficiency for the proposed methods and benchmarks on the *star* dataset.

slight miscoverage, with low variability in coverage and prediction set size, and is generally efficient relative to the benchmarks. The most competitive benchmark for providing MC guarantees is the *FWCP*.

Results across all the datasets are summarized in Table 2. We observe from the results that the proposed method *PFWCP* satisfied the posed constraint of MC above 0.9 for all the datasets, while also yielding a generally low CMC, in fact the smallest in five out of the nine datasets, and being also generally efficient, in fact the most efficient in five out of the nine datasets. The proposed one-shot methods both with and without the localized scores also perform well on some of the datasets, although the decreased flexibility of the method results in a loss of valid coverage in a few cases. Integrating the localization of the scores into the proposed framework has potential to improve the efficiency as highlighted from the results on the synthetic datasets as well as the *protein* dataset. None of the benchmarks are capable of reaching the low miscoverage and high efficiency of the proposed methods, and it is clearly seen that the low calibration data size in the cases of *CP* and *FGLCP*, due to only using local calibration data, has severe negative implications on this. Finally, the *FCP-QQ* method often fails to provide the desired coverage level, which is due to the data heterogeneity. Additional complementary results with either lessened data heterogeneity is reported in Section S4, where we have also included additional benchmarks that were omitted here for conciseness.

Calibration-conditional coverage: Results with all the benchmarks providing CCC guarantees across the datasets are summarized in Table 3, when setting the significance levels to $\alpha = 0.1$ and $\delta = 0.1$. We observe that the proposed method *PFWCP* on most of the datasets, exceptions are the *crime* and *cifar10c*, the specified CCC constraint is realized, and that the gap in CCC on the *crime* and *cifar10c* datasets is relatively small compared to gap of the other FCP benchmarks. At the same time, the proposed method *PFWCP* achieves a much lower conditional miscoverage and a much higher efficiency than the *FGLCP* benchmark, as this is limited to calibrating only with local data. The *osPFWCP* method has severe gaps in CCC showcasing the limitations due to the lessened parameter flexibility, and a similar same observation is made for the *FWCP* benchmark. On the

Table 2: Marginal coverage (MC), conditional miscoverage (CMC), and efficiency (Eff.). Methods with MC above $1 - \alpha = 0.9$, above 0.89, and below 0.89 are marked by colors green, yellow, and red, respectively. The best performing method in each dataset, that satisfy the constraint of MC above 0.9, is highlighted with boldface.

		Gaussian	Poisson	airfoil	protein	bike	concrete	crime	star	cifar10c
MC (%)	CP	89.57	89.77	89.49	89.48	89.42	89.65	89.58	89.65	89.16
	FGLCP (Min et al. 2025)	90.38	90.28	89.80	90.19	90.23	90.34	89.99	90.16	89.96
	FCP-QQ (Humbert et al. 2023)	88.70	89.97	86.48	90.20	88.20	84.17	89.11	88.78	89.40
	FWCP (Plassier et al. 2024)	90.22	89.81	92.32	90.51	89.57	89.93	89.11	89.74	85.23
	FWCP-QQ	92.13	92.34	94.06	91.09	91.10	91.78	92.11	91.82	85.87
	PFWCP	92.01	91.26	91.73	90.67	90.31	90.78	90.47	90.43	90.32
	osPFWCP	89.07	90.06	90.12	90.28	88.16	89.42	89.00	89.68	88.39
	osPFWGLCP	90.19	90.17	89.66	90.11	89.21	89.65	89.27	89.75	85.26
CMC (%)	CP	2.67	2.54	2.64	2.70	2.60	2.71	2.46	2.64	2.67
	FGLCP (Min et al. 2025)	3.36	3.45	3.58	3.51	3.25	3.44	3.36	3.47	3.52
	FedCP-QQ (Humbert et al. 2023)	2.54	1.41	3.57	1.44	2.17	5.83	1.57	1.82	2.54
	FWCP (Plassier et al. 2024)	2.37	1.66	2.51	1.32	2.04	1.58	2.94	1.76	6.52
	FWCP-QQ	2.53	2.61	4.09	1.62	1.89	2.21	2.67	2.33	6.30
	PFWCP	2.68	1.94	2.15	1.56	1.79	1.85	1.95	1.66	2.89
	osPFWCP	2.11	1.57	1.64	1.42	2.25	1.75	1.92	1.54	2.76
	osPFWGLCP	2.11	1.75	1.82	1.53	1.84	2.16	2.10	1.82	5.14
Eff.	CP	0.09	9.84	6.52	2.25	2.04	20.75	2.12	38.61	8.94
	FGLCP (Min et al. 2025)	0.09	15.96	6.73	2.36	2.45	23.14	2.29	40.10	9.00
	FedCP-QQ (Humbert et al. 2023)	0.09	9.75	5.47	2.28	1.92	15.11	2.06	36.77	8.96
	FWCP (Plassier et al. 2024)	0.09	9.71	7.49	2.31	2.03	20.72	2.15	38.27	8.55
	FWCP-QQ	0.10	12.20	8.35	2.36	2.31	22.76	2.49	43.39	8.61
	PFWCP	0.10	10.58	7.05	2.33	2.16	21.37	2.26	39.60	9.05
	osPFWCP	0.09	9.80	6.45	2.29	1.92	19.66	2.07	38.11	8.86
	osPFWGLCP	0.08	9.70	6.22	2.22	2.06	18.88	2.02	37.29	8.53

other hand, the *osPFWGLCP* method performs relatively well with just minor gaps in CCC while maintaining small conditional miscoverage and a high efficiency.

4 Conclusion

Personalized federated weighted conformal prediction closes an important gap between privacy-preserving collaboration of heterogeneous agents and reliable uncertainty quantification. By accounting for covariate shifts in both coverage bias and variance adjustments, it produces efficient prediction sets with more stable coverage compared to existing federated conformal methods. The presented framework motivates further studies to improve robustness of federated conformal prediction.

Table 3: Calibration-conditional coverage (CCC), conditional miscoverage (CMC), and efficiency (Eff.). Methods with CCC above $1 - \delta = 0.9$, above 0.8, and below 0.8 are marked by colors **green**, **yellow**, and **red**, respectively. The best performing method in each dataset, that satisfy the constraint of CCC above 0.9, is highlighted with boldface.

		Gaussian	Poisson	airfoil	protein	bike	concrete	crime	star	cifar10c
CCC (%)	CP	86.60	87.20	86.00	86.80	84.80	86.40	84.80	86.80	86.80
	FGLCP (Min et al. 2025)	90.40	93.00	91.20	90.80	90.40	91.00	89.40	90.60	91.80
	FCP-QQ (Humbert et al. 2023)	100.00	85.60	42.20	84.00	42.40	7.60	80.40	67.40	62.40
	FWCP (Plassier et al. 2024)	79.40	89.40	97.80	89.20	77.40	74.60	96.80	83.00	65.60
	FWCP-QQ	97.80	98.80	99.60	95.00	95.80	96.40	96.00	97.00	61.40
	PFWCP	99.20	96.60	97.00	92.80	91.60	91.00	85.60	92.80	88.40
	osPFWCP	93.20	90.40	88.20	87.80	63.60	77.20	69.20	81.40	77.40
	osPFWGLCP	95.00	95.60	88.00	91.80	87.40	88.40	86.20	94.80	87.80
CMC (%)	CP	3.37	3.61	3.28	3.66	3.39	3.40	3.42	3.52	3.42
	FGLCP (Min et al. 2025)	5.02	5.16	4.85	5.11	4.70	5.04	4.92	4.94	5.05
	FCP-QQ (Humbert et al. 2023)	5.89	1.99	1.60	1.80	1.41	3.37	1.68	1.62	2.28
	FWCP (Plassier et al. 2024)	2.31	2.85	4.34	1.82	2.47	1.78	6.26	2.14	4.49
	FWCP-QQ	4.29	5.05	6.32	2.63	3.68	3.58	5.97	3.64	4.54
	PFWCP	4.99	3.70	3.74	2.42	2.83	2.79	3.00	2.65	4.04
	osPFWCP	2.93	2.58	2.41	2.05	1.74	1.94	1.94	2.07	2.60
	osPFWGLCP	4.09	3.46	2.63	2.57	2.43	2.97	2.57	2.99	5.06
Eff.	CP	0.05	10.75	7.21	2.64	2.38	25.99	2.53	43.90	9.28
	FGLCP (Min et al. 2025)	0.06	22.93	9.00	2.97	3.50	35.70	3.07	47.68	9.46
	FedCP-QQ (Humbert et al. 2023)	0.05	9.72	5.94	2.45	1.96	16.81	2.22	40.15	9.05
	FWCP (Plassier et al. 2024)	0.04	10.24	7.86	2.46	2.21	21.92	3.77	41.72	9.16
	FWCP-QQ	0.05	14.61	9.39	2.55	2.64	26.08	3.78	46.32	9.11
	PFWCP	0.05	11.16	7.33	2.53	2.39	24.34	2.66	43.05	9.36
	osPFWCP	0.05	10.06	6.70	2.48	2.08	22.11	2.28	41.40	9.17
	osPFWGLCP	0.06	11.34	7.12	2.50	2.42	25.06	2.39	41.80	9.44

S1 Proofs

Proof of Proposition 1. We prove that

$$\mathbb{P}(Y \in \mathcal{C}_{\beta, \tau}^{\text{wqq}}(X) | \mathcal{D}) = \mathbb{P}(\hat{s}(X, Y) \leq Q_{\beta, \tau} | \mathcal{D}) \stackrel{d}{\rightarrow} \text{Quantile}\left(1 - \tau; \sum_{k=1}^K w_k \delta_{U_{\beta}^k}\right).$$

To that end, consider the following

$$\mathbb{P}(\hat{s}(X, Y) \leq Q_{\beta, \tau} | \mathcal{D}) = \mathbb{P}(F_{\hat{s}}^{-1}(U) \leq Q_{\beta, \tau} | \mathcal{D}) = F_{\hat{s}}(Q_{\beta, \tau}),$$

where $U \sim \text{Uniform}([0, 1])$, $F_{\hat{s}}$ is the CDF of the scores and the second equality relies on the assumption of $F_{\hat{s}}$ being continuous. What remains to show is that $F_{\hat{s}}(Q_{\beta, \tau})$ converges in distribution to the term $\text{Quantile}(1 - \tau; \sum_{k=1}^K w_k \delta_{U_{\beta}^k})$. Observe that there is an equivalence between approximating the empirical CDF and the empirical quantile. Hence, by Lemma 6, $F_{\hat{s}}(Q_{\beta}^k)$ is asymptotically distributed as $U_{\beta}^k \sim \text{Beta}((1 - \beta)(n_{\text{eff}}^k + 1), \beta(n_{\text{eff}}^k + 1))$, noting that this is the distribution of the $1 - \beta$ quantile of n_{eff}^k independent standard uniform random variables. Using that $F_{\hat{s}}^{-1}$ is nondecreasing, this implies that (Humbert et al. 2024)

$$\begin{aligned} Q_{\beta, \tau} &= \text{Quantile}\left(1 - \tau; \sum_{k=1}^K w_k \delta_{Q_{\beta}^k}\right) \stackrel{d}{\rightarrow} \text{Quantile}\left(1 - \tau; \sum_{k=1}^K w_k \delta_{F_{\hat{s}}^{-1}(U_{\beta}^k)}\right) \\ &= F_{\hat{s}}^{-1}\left(\text{Quantile}\left(1 - \tau; \sum_{k=1}^K w_k \delta_{U_{\beta}^k}\right)\right), \end{aligned}$$

concluding the proof. \square

We will now introduce some lemmas which will be required in the proof of Lemma 6. First, we state a known, elementary upper bound on Jensen's gap.

Lemma 1. Suppose that $h : \mathbb{R} \rightarrow \mathbb{R}$ is a twice differentiable convex function for which $h'' < \Lambda$ for some constant $\Lambda \in \mathbb{R}$, and let X be a real-valued random variable. Then, Jensen's gap is upper bounded by

$$\mathbb{E}[h(X)] - h(\mathbb{E}[X]) \leq \frac{1}{2} \Lambda \text{Var}[X].$$

Next we introduce Lemma 2 and Lemma 3 which are used in Lemma 6 to show that Jensen's gap, in this case, vanishes asymptotically.

Lemma 2. Let $X_j \stackrel{iid}{\sim} \mathbb{P}_X^k$ for $j \in [n]$ and some $k \in \{2, \dots, K\}$, $X \sim \mathbb{P}_X$, and $\omega(X) = [d\mathbb{P}_X/d\mathbb{P}_X^k](X)$. Assume that there exists a bounded constant $B > 0$ such that $\mathbb{P}_X(\omega(X) \leq B) = 1$ and $\mathbb{P}_X^k(\omega(X_j) \leq B) = 1$ for $j \in [n]$. Then, $\text{Var}[\sum_{j=1}^n \omega(X_j) + \omega(X)] = O(n)$.

Proof. Consider the following which holds by independence of X_j :

$$\text{Var}\left[\sum_{j=1}^n \omega(X_j) + \omega(X)\right] = \sum_{j=1}^n \text{Var}[\omega(X_j)] + \text{Var}[\omega(X)]$$

By identical distribution of X_j ,

$$\text{Var}\left[\sum_{j=1}^n \omega(X_j) + \omega(X)\right] = n(\mathbb{E}[\omega^2(X_1)] - \mathbb{E}[\omega(X_1)]^2) + \mathbb{E}[\omega^2(X)] - \mathbb{E}[\omega(X)]^2.$$

Finally, almost sure boundedness of the weights implies that $\mathbb{E}[\omega(X_1)] \leq B$ and $\mathbb{E}[\omega^2(X_1)] \leq B^2$, which concludes the proof. \square

Lemma 3. Let $X_j \sim \mathbb{P}_X^k$ for $j = 1, \dots, n$ and some $k \in \{2, \dots, K\}$, $X \sim \mathbb{P}_X$, and $\omega(X) = [d\mathbb{P}_X/d\mathbb{P}_X^k](X)$. Assume that there exist bounded constants $0 < A \leq 1 \leq B$ such that $\mathbb{P}_X(\omega(X) \in [A, B]) = 1$ and $\mathbb{P}_X^k(\omega(X_j) \in [A, B]) = 1$. Then, the smallest constant Λ_n , such that for any given n ,

$$\mathbb{P}\left(\left(\sum_{j=1}^n \omega(X_j) + \omega(X)\right)^{-d} < \Lambda_n\right) = 1$$

is of order $O(1/n^d)$ for $d \geq 1$.

Proof. As $\omega(X) \in [A, B]$ almost surely

$$\mathbb{P}\left(\sum_{j=1}^n \omega(X_j) + \omega(X) \geq A(n+1)\right) = 1,$$

and so

$$\mathbb{P}\left(\left(\sum_{j=1}^n \omega(X_j) + \omega(X)\right)^{-d} \leq A^{-d}(n+1)^{-d}\right) = 1$$

Hence, Λ_n is necessarily upper bounded by $A^{-d}(n+1)^{-d}$. Similarly, Λ_n is lower bounded by $B^{-d}(n+1)^{-d}$, concluding the proof. \square

The final lemmas before proceeding to the proof of Lemma 6 provides statements related to the convergence of the normalization factor $\sum_{j=1}^n \omega(X_j) + \omega(X)$ and the effective sample size $\|\omega(X_1), \dots, \omega(X_n)\|_1^2 / \|\omega(X_1), \dots, \omega(X_n)\|_2^2$ when replacing a calibration datum with a test datum. These results will be necessary to apply McDiarmid's tail bound in the proof of Lemma 6.

Lemma 4. Let $X_j \sim \mathbb{P}_X^k$ for $j = 1, \dots, n$ and some $k \in \{2, \dots, K\}$, $\tilde{X}, X \sim \mathbb{P}_X$, and $\omega(X) = [d\mathbb{P}_X/d\mathbb{P}_X^k](X)$. Assume that there exists bounded constants $0 < A \leq 1 \leq B$ such that $\mathbb{P}_X(\omega(X) \in [A, B]) = 1$ and $\mathbb{P}_X^k(\omega(X_j) \in [A, B]) = 1$. Then, as $n \rightarrow \infty$

$$\mathbb{P}\left(\left|\frac{1}{\sum_{j=1}^n \omega(X_j) + \omega(X)} - \frac{1}{\sum_{j=2}^n \omega(X_j) + \omega(\tilde{X}) + \omega(X)}\right| > \epsilon\right) \rightarrow 0,$$

for any $\epsilon > 0$.

Proof. First, notice that almost surely

$$\begin{aligned} & \left| \frac{1}{\sum_{j=1}^n \omega(X_j) + \omega(X)} - \frac{1}{\sum_{j=2}^n \omega(X_j) + \omega(\tilde{X}) + \omega(X)} \right| \\ &= \left| \frac{\omega(\tilde{X}) - \omega(X_1)}{\left(\sum_{j=1}^n \omega(X_j) + \omega(X)\right) \left(\sum_{j=2}^n \omega(X_j) + \omega(\tilde{X}) + \omega(X)\right)} \right| \\ &\leq \frac{B - A}{A^2(n+1)^2}. \end{aligned}$$

It follows that

$$\mathbb{P}\left(\left|\frac{1}{\sum_{j=1}^n \omega(X_j) + \omega(X)} - \frac{1}{\sum_{j=2}^n \omega(X_j) + \omega(\tilde{X}) + \omega(X)}\right| > \epsilon\right) \leq \mathbb{P}\left(\frac{B - A}{A^2(n+1)^2} > \epsilon\right).$$

The probability of the trivial event $\frac{B-A}{A^2(n+1)^2} > \epsilon$ goes to zero when $\frac{B-A}{A^2(n+1)^2} \rightarrow 0$ which occurs as $n \rightarrow \infty$. \square

Lemma 5. Let $X_j \sim \mathbb{P}_X^k$ for $j = 1, \dots, n$ and some $k \in \{2, \dots, K\}$, $X \sim \mathbb{P}_X$, and $\omega(X) = [d\mathbb{P}_X/d\mathbb{P}_X^k](X)$. Assume that there exists bounded constants $0 < A \leq 1 \leq B$ such that $\mathbb{P}_X(\omega(X) \in [A, B]) = 1$ and $\mathbb{P}_X^k(\omega(X_j) \in [A, B]) = 1$. Then, as $n \rightarrow \infty$

$$\mathbb{P}\left(\left|\frac{\|\omega(X_1), \dots, \omega(X_n)\|_2^2}{\|\omega(X_1), \dots, \omega(X_n)\|_1^2} - \frac{\|\omega(X), \omega(X_2), \dots, \omega(X_n)\|_2^2}{\|\omega(X), \omega(X_2), \dots, \omega(X_n)\|_1^2}\right| > \epsilon\right) \rightarrow 0,$$

for any $\epsilon > 0$.

Proof. The result follows from similar arguments as for Lemma 4. \square

We are now ready to present the core technical lemma used in the proof of Proposition 1.

Lemma 6. Let $(X_i, Y_i) \stackrel{iid}{\sim} \mathbb{P}^k = \mathbb{P}_{Y|X} \mathbb{P}_X^k$ for $i \in [n]$ and some $k \in \{2, \dots, K\}$ and $(X, Y), (X_i^{\text{te}}, Y_i^{\text{te}}) \sim \mathbb{P} = \mathbb{P}_{Y|X} \mathbb{P}_X$. Let $\hat{s}_i^{\text{te}} = \hat{s}(X_i^{\text{te}}, Y_i^{\text{te}})$ and $\hat{s}_i = \hat{s}(X_i, Y_i)$ be pre-trained scores. Assuming that \mathbb{P}_X is absolutely continuous with respect to \mathbb{P}_X^k , let $\omega(X) = [d\mathbb{P}_X/d\mathbb{P}_X^k](X)$ be the density ratio, and assume further that there exists bounded constants $0 < A \leq 1 \leq B$ such that $\mathbb{P}_X(\omega(X) \in [A, B]) = 1$ and $\mathbb{P}_X^k(\omega(X_i) \in [A, B]) = 1$. Moreover, denote by $n_{\text{eff}} = \lceil \frac{\|\omega(X_1), \dots, \omega(X_n)\|_1^2}{\|\omega(X_1), \dots, \omega(X_n)\|_2^2} \rceil$ the effective sample size. Then, as $n \rightarrow \infty$,

$$\sup_{W \in \sigma(\mathbb{R})} \left| \frac{\sum_{i=1}^n \omega(X_i) \delta_{\hat{s}_i}(W) + \omega(X) \delta_{\infty}(W)}{\sum_{i=1}^n \omega(X_i) + \omega(X)} - \frac{\sum_{i=1}^{n_{\text{eff}}} \delta_{\hat{s}_i^{\text{te}}}(W) + \delta_{\infty}(W)}{n_{\text{eff}} + 1} \right| \rightarrow 0,$$

where $\sigma(\mathbb{R})$ denotes the set of left-infinite half intervals $W = (-\infty, x]$.

Proof. The proof is inspired by the proof of Lemma 8.5 of [Gretton et al. \(2009\)](#). Before proceeding with the proof, consider the following shorthand notations: $Z_j = (X_j, Y_j)$, $Z_j^{\text{te}} = (X_j^{\text{te}}, Y_j^{\text{te}})$, $\tilde{Z} = (\tilde{X}, \tilde{Y})$, $\tilde{Z} = (\tilde{X}, \tilde{Y})$, $\omega = \omega(X)$, $\omega_j = \omega(X_j)$, $\tilde{\omega} = \omega(\tilde{X})$, $\tilde{\omega} = \omega(\tilde{X})$, $\omega_{1:n} = [\omega_1, \dots, \omega_n]$, $\delta_j = \delta_{\tilde{s}(Z_j)}$, $\tilde{\delta} = \delta_{\tilde{s}(\tilde{Z})}$, $\check{\delta} = \delta_{\check{s}(\check{Z})}$, $N = N(X_1, \dots, X_n, X) = \sum_{j=1}^n \omega_j + \omega$, $M = M(X_1, \dots, X_n) = n_{\text{eff}} + 1$, and $NM(X_1, \dots, X_n, X) = N(X_1, \dots, X_n, X)M(X_1, \dots, X_n)$. Defining also the following shorthand expressions: $\Delta = \Delta(Z_1, \dots, Z_n, X) = \frac{1}{N} \left(\sum_{i=1}^n \omega_i \delta_i(W) + \omega \delta_\infty(W) \right)$ for any $W \in \sigma(\mathbb{R})$, $\Delta^{\text{te}} = \Delta^{\text{te}}(Z_1, \dots, Z_n, Z_1^{\text{te}}, \dots, Z_{M-1}^{\text{te}}) = \frac{1}{M} \left(\sum_{i=1}^{M-1} \delta_i^{\text{te}}(W) + \delta_\infty(W) \right)$, and $\Xi = \Xi(Z_1, \dots, Z_n, X, Z_1^{\text{te}}, \dots, Z_{M-1}^{\text{te}}) = |\Delta - \Delta^{\text{te}}|$. We will apply McDiarmid's tail bound ([McDiarmid 1989](#)) to show that

$$\mathbb{P} \left(\sup_W |\Xi - \mathbb{E}[\Xi]| > \epsilon \right) < 2 \exp \left(\frac{-2\epsilon^2}{\sum_{i=1}^{n+M} c_i^2} \right),$$

for any $\epsilon > 0$ and where c_i are such that $\sup_W |\Xi - \Xi_{-i}| \leq c_i$ where $\Xi_{-i} = \Xi(Z_1, \dots, Z_{i-1}, \tilde{Z}, Z_{i+1}, \dots, Z_n, X, Z_1^{\text{te}}, \dots, Z_{M-1}^{\text{te}})$ for $i \in [n+M]$. For this we need to bound the change in Ξ if we replace any (X_i, Y_i) by an arbitrary $\tilde{Z} = (\tilde{X}, \tilde{Y})$ and likewise if we replace any $(X_i^{\text{te}}, Y_i^{\text{te}})$ by some $\tilde{Z} = (\tilde{X}, \tilde{Y})$. For $i \in [n]$, by the triangle inequality,

$$\sup_W |\Xi - \Xi_{-i}| = \sup_W |\Delta - \Delta^{\text{te}} - (\Delta_{-i} - \Delta_{-i}^{\text{te}})| \leq \sup_W |\Delta - \Delta_{-i}| + |\Delta^{\text{te}} - \Delta_{-i}^{\text{te}}|,$$

where $\Delta_{-i} = \Delta(Z_1, \dots, Z_{i-1}, \tilde{Z}, Z_{i+1}, \dots, Z_n, X)$ for $i \in [n+1]$, and $\Delta_{-i}^{\text{te}} = \Delta^{\text{te}}(Z_1, \dots, Z_n, Z_1^{\text{te}}, \dots, Z_{i-n-2}^{\text{te}}, \tilde{Z}, Z_{i-n}^{\text{te}}, \dots, Z_{M-1}^{\text{te}})$ for $i \in [n+M] \setminus \{n+1\}$. For $i \in [n+1]$, define $\Delta_N^i = \tilde{\omega} - \omega_i$, and consider the first term

$$\begin{aligned} \sup_W |\Delta - \Delta_{-i}| &= \sup_W \left| \frac{1}{N} \left(\sum_{j=1}^n \omega_j \delta_j(W) + \omega \delta_\infty(W) \right) \right. \\ &\quad \left. - \frac{1}{N + \Delta_N^i} \left(\sum_{j=1, j \neq i}^n \omega_j \delta_j(W) + \tilde{\omega} \tilde{\delta}(W) + \omega \delta_\infty(W) \right) \right|. \end{aligned}$$

By the boundedness of the weights and using Lemma 4, for $\epsilon' > 0$ there exists n' such that for $n \geq n'$ it holds that $|1/N - 1/(N + \Delta_N^i)| < \epsilon'$. With this, for n sufficient large

$$\sup_W |\Delta - \Delta_{-i}| = \frac{1}{N} \sup_W \left| \omega_i \delta_i(W) - \omega(\tilde{X}) \tilde{\delta}(W) \right| + O(\epsilon') = O(1/n) + O(\epsilon').$$

Define now $M_{-i} = M(X_1, \dots, X_{-i}, \tilde{X}, X_i + 1, \dots, X_n)$ for $i \in [n]$, let

$$\Delta_M^i(W) = \mathbb{1}[M_{-i} \geq M] \sum_{j=M}^{M_{-i}-1} \delta_j^{\text{te}}(W) + \mathbb{1}[M_{-i} < M] \sum_{j=M-i}^{M-1} \delta_j^{\text{te}}(W),$$

denote by $m(W) = \sum_{j=1}^{M-1} \delta_j^{\text{te}}(W) + \delta_\infty(W)$, and consider the second term

$$\sup_W |\Delta^{\text{te}} - \Delta_{-i}^{\text{te}}| = \sup_W \left| \frac{m(W)}{M} - \frac{m(W) + \Delta_M^i(W)}{M + \Delta_M^i(\mathbb{R})} \right| = \sup_W \left| \frac{m(W) \Delta_M^i(W)}{M(M + \Delta_M^i(\mathbb{R}))} - \frac{\Delta_M^i(W)}{M + \Delta_M^i(\mathbb{R})} \right|.$$

By the boundedness of the weights and using Lemma 5, for any $\epsilon'' > 0$ there exists n'' such that for $n \geq n''$ it holds that $|1/M - 1/(M + \Delta_M^i(\mathbb{R}))| < \epsilon''$. Hence, for n sufficiently large

$$\sup_W |\Delta^{\text{te}} - \Delta_{-i}^{\text{te}}| = \sup_W \left| \frac{m(W) \Delta_M^i(W)}{M(M + \Delta_M^i(\mathbb{R}))} - \frac{\Delta_M^i(W)}{M + \Delta_M^i(\mathbb{R})} \right| + O(\epsilon'') = O(1/n) + O(\epsilon'').$$

Combining the terms we can conclude that for $i \in [n]$, for n sufficient large $\sup_W |\Xi - \Xi_{-i}| = O(1/n) + O(\epsilon') + O(\epsilon'')$. Similarly, for $i = n+1$, $\sup_W |\Xi - \Xi_{-i}| = O(1/n) + O(\epsilon')$.

For $i \in \{n+2, \dots, n+M\}$, we have

$$\begin{aligned} \sup_W |\Xi - \Xi_{-i}| &= \sup_W |\Delta - \Delta^{\text{te}} - (\Delta - \Delta_{-i}^{\text{te}})| = \sup_W |\Delta^{\text{te}} - \Delta_{-i}^{\text{te}}| \\ &= \frac{1}{M} \sup_W \left| \delta_{i-n-1}^{\text{te}}(W) - \tilde{\delta}(W) \right| = O(1/n). \end{aligned}$$

Applying now McDiarmid's tail bound, for n sufficiently large, it holds that

$$\mathbb{P}\left(\sup_W |\Xi - \mathbb{E}[\Xi]| > \epsilon\right) < 2\exp(-2\epsilon^2 n / c_{\epsilon', \epsilon''}),$$

for some constant $c_{\epsilon', \epsilon''} > 0$. Hence, with probability $1 - \delta$ the deviation of the random variable from its expectation is bounded by

$$\sup_W |\Xi - \mathbb{E}[\Xi]| \leq \sqrt{\frac{-c_{\epsilon', \epsilon''} \ln(\delta/2)}{2n}}.$$

We proceed to bound the expected value $\mathbb{E}[\Xi]$ using Jensen's inequality as $\mathbb{E}[\Xi] \leq \sqrt{\mathbb{E}[\Xi^2]}$. Expanding the expectation

$$\begin{aligned} \sup_W \mathbb{E}[\Xi^2] &= \sup_W \mathbb{E}\left[\left(\frac{1}{N} \left(\sum_{j=1}^n \omega_j \delta_{s_j} + \omega \delta_\infty\right) - \frac{1}{M} \left(\sum_{j=1}^{M-1} \delta_{s_j^{\text{te}}} + \delta_\infty\right)\right)^2\right] \\ &= \sup_W \mathbb{E}\left[\frac{1}{N^2} \left(\sum_{i,j=1}^n \omega_i \omega_j \delta_i \delta_j + 2 \sum_{j=1}^n \omega_j \omega \delta_j \delta_\infty + \omega^2 \delta_\infty \delta_\infty\right)\right] \\ &\quad + \mathbb{E}\left[\frac{1}{M^2} \left(\sum_{i,j=1}^{M-1} \delta_i^{\text{te}} \delta_j^{\text{te}} + 2 \sum_{j=1}^{M-1} \delta_j^{\text{te}} \delta_\infty + \delta_\infty \delta_\infty\right)\right] \\ &\quad - 2\mathbb{E}\left[\frac{1}{NM} \left(\sum_{i=1}^n \sum_{j=1}^{M-1} \omega_i \delta_i \delta_j^{\text{te}} + \sum_{i=1}^n \omega_i \delta_i \delta_\infty + \sum_{j=1}^{M-1} \omega \delta_j^{\text{te}} \delta_\infty + \omega \delta_\infty \delta_\infty\right)\right]. \end{aligned} \tag{5}$$

Beginning with the first term, using the law of total expectation, and interchanging measures exploiting that $\mathbb{P}_X(X) = \omega(X) \mathbb{P}_X^k(X)$:

$$\begin{aligned} \sup_W \mathbb{E}\left[\frac{1}{N^2} \sum_{i,j=1}^n \omega_i \omega_j \delta_i \delta_j\right] &= \sup_W n(n-1) \mathbb{E}\left[\mathbb{E}\left[\frac{\tilde{\delta}^{\text{te}} \check{\delta}^{\text{te}}}{N^2(\tilde{X}^{\text{te}}, \check{X}^{\text{te}}, X_3, \dots, X_n, X)} \mid X_3, \dots, X_n, X\right]\right] \\ &\quad + n \mathbb{E}\left[\mathbb{E}\left[\frac{\tilde{\omega}^{\text{te}} \tilde{\delta}^{\text{te}} \check{\delta}^{\text{te}}}{N^2(\tilde{X}^{\text{te}}, X_2, \dots, X_n, X)} \mid X_2, \dots, X_n, X\right]\right] \\ &= \sup_W (n^2 - n) \mathbb{E}\left[\frac{\tilde{\delta}^{\text{te}} \check{\delta}^{\text{te}}}{N^2(\tilde{X}^{\text{te}}, \check{X}^{\text{te}}, X_3, \dots, X_n, X)}\right] \\ &\quad + n \mathbb{E}\left[\frac{\tilde{\omega}^{\text{te}} \tilde{\delta}^{\text{te}} \check{\delta}^{\text{te}}}{N^2(\tilde{X}^{\text{te}}, X_2, \dots, X_n, X)}\right] \\ &\leq (n^2 - n) \mathbb{E}\left[\frac{1}{N^2(\tilde{X}^{\text{te}}, \check{X}^{\text{te}}, X_3, \dots, X_n, X)}\right] \\ &\quad + n \mathbb{E}\left[\frac{\tilde{\omega}^{\text{te}}}{N^2(\tilde{X}^{\text{te}}, X_2, \dots, X_n, X)}\right]. \end{aligned}$$

Moving on to the first term in the second line of Eq. (5):

$$\begin{aligned} \sup_W \mathbb{E}\left[\frac{1}{M^2} \sum_{i,j=1}^{M-1} \delta_i^{\text{te}} \delta_j^{\text{te}}\right] &= \sup_W \mathbb{E}\left[\frac{1}{M^2} \left(\sum_{j=1}^{M-1} \mathbb{E}[\delta_j^{\text{te}} \delta_j^{\text{te}} \mid X_1, \dots, X_n] + \sum_{\substack{i,j=1 \\ j \neq i}}^{M-1} \mathbb{E}[\delta_i^{\text{te}} \delta_j^{\text{te}} \mid X_1, \dots, X_n]\right)\right] \\ &= \sup_W \mathbb{E}\left[\frac{1}{M} - \frac{1}{M^2}\right] \mathbb{E}[\delta_1^{\text{te}} \delta_1^{\text{te}}] + \mathbb{E}\left[1 - \frac{3}{M} + \frac{2}{M^2}\right] \mathbb{E}[\delta_1^{\text{te}} \delta_2^{\text{te}}] \\ &\leq \mathbb{E}\left[\frac{1}{M^2}\right] - 2\mathbb{E}\left[\frac{1}{M}\right] + 1. \end{aligned} \tag{6}$$

Now the first term in the third line of Eq. (5):

$$\begin{aligned}
\sup_W 2\mathbb{E}\left[\frac{1}{NM} \sum_{i=1}^n \sum_{j=1}^{M-1} \omega_i \delta_i, \delta_j^{\text{te}}\right] &= \sup_W 2n\mathbb{E}\left[\frac{\sum_{j=1}^{M(\tilde{X}^{\text{te}}, X_2, \dots, X_n)-1} \tilde{\delta}^{\text{te}} \delta_j^{\text{te}}}{NM(\tilde{X}^{\text{te}}, X_2, \dots, X_n, X)}\right] \\
&= \sup_W 2n\mathbb{E}\left[\frac{(M(\tilde{X}^{\text{te}}, X_2, \dots, X_n) - 1)\tilde{\delta}^{\text{te}} \delta_1^{\text{te}}}{NM(\tilde{X}^{\text{te}}, X_2, \dots, X_n, X)}\right] \\
&\leq 2n\left(\mathbb{E}\left[\frac{1}{N(\tilde{X}^{\text{te}}, X_2, \dots, X_n, X)}\right]\right. \\
&\quad \left. + \mathbb{E}\left[\frac{1}{NM(\tilde{X}^{\text{te}}, X_2, \dots, X_n, X)}\right]\right).
\end{aligned}$$

What remains is to argue that the terms $\mathbb{E}\left[\frac{n^2}{N^2(\tilde{X}^{\text{te}}, \check{X}^{\text{te}}, X_3, \dots, X_n, X)}\right]$ and $\mathbb{E}\left[\frac{-2n}{N(\tilde{X}^{\text{te}}, X_2, \dots, X_n, X)}\right]$ cancels with the 1 of Eq. (6). With Jensen's inequality we obtain that

$$\begin{aligned}
\mathbb{E}\left[\frac{n}{N(\tilde{X}^{\text{te}}, X_2, \dots, X_n, X)}\right] &\geq \frac{n}{\mathbb{E}[N(\tilde{X}^{\text{te}}, X_2, \dots, X_n, X)]} = \frac{n}{2\mathbb{E}[\tilde{\omega}^{\text{te}}] + (n-1)\mathbb{E}[\omega_2]} \\
&= \frac{n}{2\mathbb{E}[\tilde{\omega}^{\text{te}}] + (n-1)}.
\end{aligned}$$

By regularity of the weight function, $\mathbb{E}[\tilde{\omega}^{\text{te}}]$ is bounded and hence $n/(2\mathbb{E}[\tilde{\omega}^{\text{te}}] + (n-1)) \rightarrow 1$ as $n \rightarrow \infty$. Jensen's gap can be bounded by second order properties, see Lemma 1,

$$\left|\mathbb{E}\left[\frac{n}{N(\tilde{X}^{\text{te}}, X_2, \dots, X_n, X)}\right] - \frac{n}{2\mathbb{E}[\tilde{\omega}^{\text{te}}] + (n-1)}\right| \leq \left|\frac{n}{2}\Lambda_n \text{Var}[N(\tilde{X}^{\text{te}}, X_2, \dots, X_n, X)]\right|,$$

where $\Lambda_n > 0$ is the smallest constant such that for a given n , then $\mathbb{P}\left(\frac{2}{N^3(\tilde{X}^{\text{te}}, X_2, \dots, X_n, X)} < \Lambda_n\right) = 1$. As $\omega(X_i) \in [A, B]$ almost surely, $\Lambda_n = O(1/n^3)$, see Lemma 3. Further, from Lemma 2, $\text{Var}[N(\tilde{X}^{\text{te}}, X_2, \dots, X_n, X)] = O(n)$. Hence, Jensen's gap is upper bounded by a term that converges to zero as $n \rightarrow \infty$. This implies that $\mathbb{E}[n/N(\tilde{X}^{\text{te}}, X_2, \dots, X_n, X)] \rightarrow 1$ as $n \rightarrow \infty$. Repeating the same arguments

$$\begin{aligned}
\mathbb{E}\left[\frac{n^2}{N^2(\tilde{X}^{\text{te}}, \check{X}^{\text{te}}, X_3, \dots, X_n, X)}\right] &\geq \frac{n^2}{\mathbb{E}[N(\tilde{X}^{\text{te}}, \check{X}^{\text{te}}, X_3, \dots, X_n, X)]^2} \\
&= \frac{n^2}{(3\mathbb{E}[\tilde{\omega}^{\text{te}}] + (n-2)\mathbb{E}[\omega_2])^2} \\
&= \frac{n^2}{(3\mathbb{E}[\tilde{\omega}^{\text{te}}] + (n-2))^2}.
\end{aligned}$$

By the almost surely boundedness of the weight function, $\mathbb{E}[\tilde{\omega}^{\text{te}}]$ is bounded and hence $n^2/(3\mathbb{E}[\tilde{\omega}^{\text{te}}] + (n-2))^2 \rightarrow 1$ as $n \rightarrow \infty$. Jensen's gap can be bounded by second order properties

$$\begin{aligned}
\left|\mathbb{E}\left[\frac{n^2}{N^2(\tilde{X}^{\text{te}}, \check{X}^{\text{te}}, X_3, \dots, X_n, X)}\right] - \frac{n^2}{(3\mathbb{E}[\tilde{\omega}^{\text{te}}] + (n-2))^2}\right| \\
\leq \left|\frac{n^2}{2}\Lambda'_n \text{Var}[N(\tilde{X}^{\text{te}}, \check{X}^{\text{te}}, X_3, \dots, X_n, X)]\right|,
\end{aligned}$$

where $\Lambda'_n > 0$ is the smallest constant such that for a given n , then $\mathbb{P}\left(\frac{6}{N^4(\tilde{X}^{\text{te}}, \check{X}^{\text{te}}, X_3^{\text{tr}}, \dots, X_n^{\text{tr}}, X)} < \Lambda'_n\right) = 1$. By regularity of the weight function and using Lemma 3, $\Lambda_n = O(1/n^4)$, and additionally, using Lemma 2, $\text{Var}[N(\tilde{X}^{\text{te}}, \check{X}^{\text{te}}, X_3, \dots, X_n, X)] = O(n)$. Hence, Jensen's gap is upper bounded by a term that converges to zero as $n \rightarrow \infty$. This implies that $\mathbb{E}[n^2/N^2(\tilde{X}^{\text{te}}, \check{X}^{\text{te}}, X_3, \dots, X_n, X)] \rightarrow 1$ as $n \rightarrow \infty$.

The remaining terms in Eq. (5) are quickly observed to be of order $\mathbb{E}[1/N]$, $\mathbb{E}[1/M]$, $\mathbb{E}[1/N^2]$ or $\mathbb{E}[1/M^2]$, and by almost surely boundedness of the weights, each of these terms are either of order $1/n$ or $1/n^2$.

Combining the bound on the expected value and the tail bound implies the result. \square

S2 Designing the weights

The methodology presented in Section 2 relies on two levels of weights: the local weights $\hat{\omega}^k$ meant to approximate the density ratio $d\mathbb{P}_X/d\mathbb{P}_X^k$, and the aggregation weights w_k meant to measure distribution similarity.

Density ratio weights: Density ratios play a central role in the context of distribution shifts in machine learning (Huang et al. 2006, Sugiyama et al. 2007, 2008, Gretton et al. 2009, Tibshirani et al. 2019), and estimation of density ratios is in itself a large and active research field (Nguyen et al. 2007, Sugiyama et al. 2012, Choi et al. 2022, Yu et al. 2025).

In this paper, we use the method also applied by Tibshirani et al. (2019). The idea is that

$$\frac{\mathbb{P}(X \sim \mathbb{P}_X | X = x)}{\mathbb{P}(X \sim \mathbb{P}_X^k | X = x)} = \frac{\mathbb{P}(X \sim \mathbb{P}_X)}{\mathbb{P}(X \sim \mathbb{P}_X^k)} \frac{d\mathbb{P}_X}{d\mathbb{P}_X^k}(x),$$

hence, the weight $\mathbb{P}(X \sim \mathbb{P}_X | X = x)/\mathbb{P}(X \sim \mathbb{P}_X^k | X = x)$ is proportional to the density ratio $[d\mathbb{P}_X/d\mathbb{P}_X^k](x)$. A model trained to solve the binary classification problem of determining if an input covariate X is sampled from \mathbb{P}_X or \mathbb{P}_X^k , with soft output scores $\hat{g}^k : \mathcal{X} \rightarrow (0, 1)$, exactly provides an estimate of $\mathbb{P}(X \sim \mathbb{P}_X | X = x)$. Such a model can be fitted to the training data $\{(\tilde{X}_i^k, 0)\}_{i=1}^{\tilde{n}_k} \cup \{(\tilde{X}_i^1, 1)\}_{i=1}^{\tilde{n}_1}$. Hence, we may estimate the density ratio weights (up to proportionality) by $\hat{\omega}^k(X) = \hat{g}^k(X)/(1 - \hat{g}^k(X))$. Employing this approach allows for a highly flexible solution: depending on the data, the practitioner may select a suitable model for the binary classification problem. In this work, we limited our attention to fully connected neural networks, since this provides a powerful approximator well-suited for a wide variety of datasets.

If each of the K participating DAs require calibration, the method described above in fact requires $K(K-1)/2$ distinct binary classifiers, one for each of the pair-wise density ratios, $[d\mathbb{P}_X^k/d\mathbb{P}_X^{k'}](x)$ for $k, k' \in [K], k \neq k'$. There is another possible solution which only requires a total of K binary classifiers. The idea is that

$$\frac{\mathbb{P}(X \sim \mathbb{P}_X^k | X = x)}{\mathbb{P}(X \sim \mathbb{P}_X^{k'} | X = x)} = \frac{\mathbb{P}(X \sim \mathbb{P}_X^k | X = x)}{\mathbb{P}(X \sim \sum_{j=1}^K \mathbb{P}_X^j | X = x)} \frac{\mathbb{P}(X \sim \sum_{j=1}^K \mathbb{P}_X^j | X = x)}{\mathbb{P}(X \sim \mathbb{P}_X^{k'} | X = x)}.$$

The density ratio $\mathbb{P}(X \sim \mathbb{P}_X^k | X = x)/\mathbb{P}(X \sim \sum_{j=1}^K \mathbb{P}_X^j | X = x)$ can be estimated by training a binary classifier on $(\{(\tilde{X}_i^k, 1)\}_{i=1}^{\tilde{n}_k} \cup \{(\tilde{X}_i^k, 0)\}_{i=\ell+1}^{\tilde{n}_k}) \cup (\bigcup_{k' \neq k} \{(\tilde{X}_i^{k'}, 0)\}_{i=1}^{\tilde{n}_{k'}})$ with appropriate training data weighting, for $\ell \in [\tilde{n}_k]$, yielding soft output scores $\hat{\varrho}^k : \mathcal{X} \rightarrow (0, 1)$, thereby designing the density ratio weights (up to proportionality) by

$$\hat{\omega}^k(X) = \frac{\hat{\varrho}^1(X)(1 - \hat{\varrho}^k(X))}{\hat{\varrho}^k(X)(1 - \hat{\varrho}^1(X))}.$$

Another potential solution is multi-class classification. In such a setting, a model is trained on data, $\bigcup_{k=1}^K \{(\tilde{X}_i^k, e_k)\}_{i=1}^{\tilde{n}_k}$ where e_k is the vector with 0 elements except an entry of 1 in the k -th entry, yielding soft output scores $\hat{\rho} : \mathcal{X} \rightarrow (0, 1)^K$ with $\sum_{k=1}^K \hat{\rho}_k = 1$. Here, $\hat{\rho}_k$ is an estimate of $\mathbb{P}(X \sim \mathbb{P}_X^k | X = x)$, and the density ratios are estimated as $\hat{\omega}^k = \hat{\rho}_1/\hat{\rho}_k$ for $k \in \{2, \dots, K\}$. The downside of this approach is that learning a multi-class classifier is more challenging than learning a binary classifier.

The methods described above falls into the category of probabilistic classification approaches. Other methods include moment matching (Huang et al. 2006), and minimization of distribution divergences (Nguyen et al. 2007), see also Sugiyama et al. (2012) for a detailed review.

Distribution similarity weights: The aggregation weights, w_k , can be used to provide more weight to calibration information from DAs with a higher distribution similarity. In this paper, for simplicity and to avoid additional communication overhead, we used $w_k \propto n_{\text{eff}}^k$. However, a plethora of other options could be investigated, including distribution divergence measures such as the Kullback-Leibler divergence, distribution distance metrics such as the Wasserstein metric, relative divergence measures (Yamada et al. 2011), and outlier distribution factors (Perini et al. 2023, Vejling et al. 2026).

Consider as an example the Kullback-Leibler divergence

$$\text{KL}(\mathbb{P}_X, \mathbb{P}_X^k) = \int \log([\text{d}\mathbb{P}_X/\text{d}\mathbb{P}_X^k](X)) \text{d}\mathbb{P}_X(X).$$

Computing the Kullback-Leibler divergence is non-trivial in practice and also has the downside of being non-symmetric in its arguments. Further, convergence rates of estimators is slow, and a more reliable solution is relative divergence measures proposed by [Yamada et al. \(2011\)](#). Here, the divergence between \mathbb{P}_X and $(1-\epsilon)\mathbb{P}_X + \epsilon\mathbb{P}_X^k$ for $0 < \epsilon \leq 1$ is considered, and this provably improves convergence rates ([Yamada et al. 2011](#)). Another approach is based on outlier distribution factors. Here, the distribution \mathbb{P}_X^k is expressed as a mixture between \mathbb{P}_X and a proper outlier distribution \mathbb{Q}_X^k , see [Blanchard et al. \(2010\)](#), specifically, $\mathbb{P}_X^k = (1 - \pi)\mathbb{P}_X + \pi\mathbb{Q}_X^k$ for an outlier factor $0 < \pi \leq 1$. The outlier factor directly provides a measure of distribution similarity and there exists practical methods for estimating it ([Perini et al. 2023](#), [Vejling et al. 2026](#)).

S3 Additional data and implementation details

S3.1 Details regarding datasets

Synthetic Gaussian data: This synthetic data is generated by sampling covariates $X_i^k \stackrel{iid}{\sim} \mathcal{N}(\gamma_k, 1)$ for the k -th data agent where $\gamma_k \in \mathbb{R}^d$ and $d = 10$ is the dimensionality. The response variable is defined as $Y_i^k = \sum_{l=1}^d [X_i^k]_l$. We evaluate three setting with varying degrees of data heterogeneity. In the severe case, data heterogeneity is simulated by sampling $[\gamma_1]_l \stackrel{iid}{\sim} \text{Uniform}([-1, -0.5]) \mathbb{1}[l \leq \lfloor d/4 \rfloor]$ for $l \in [d]$ and $[\gamma_k]_l \stackrel{iid}{\sim} \text{Uniform}([-0.7, 0.7]) \mathbb{1}[l > \lfloor d/4 \rfloor]$ for $k \in \{2, \dots, K\}$ and $l \in [d]$. In the moderate case, data heterogeneity is simulated by sampling $[\gamma_1]_l \stackrel{iid}{\sim} \text{Uniform}([-0.5, -0.25]) \mathbb{1}[l \leq \lfloor d/4 \rfloor]$ for $l \in [d]$ and $[\gamma_k]_l \stackrel{iid}{\sim} \text{Uniform}([-0.35, 0.35]) \mathbb{1}[l > \lfloor d/4 \rfloor]$ for $k \in \{2, \dots, K\}$ and $l \in [d]$. In the mild case, data heterogeneity is simulated by sampling $[\gamma_1]_l \stackrel{iid}{\sim} \text{Uniform}([-0.25, -0.125]) \mathbb{1}[l \leq \lfloor d/4 \rfloor]$ for $l \in [d]$ and $[\gamma_k]_l \stackrel{iid}{\sim} \text{Uniform}([-0.175, 0.175]) \mathbb{1}[l > \lfloor d/4 \rfloor]$ for $k \in \{2, \dots, K\}$ and $l \in [d]$. The density ratios $[\text{d}\mathbb{P}/\text{d}\mathbb{P}^k](X)$ are known as ratios of Gaussian densities, which allows for the use of oracle weights in the numerical experiments. The severe case is the one studied in [Section 3](#).

Synthetic Poisson data: This synthetic data is generated by sampling covariates $X_i^k \stackrel{iid}{\sim} \mathcal{N}(3 + \gamma_k, 1)$ for the k -th data agent where $\gamma_k \in \mathbb{R}^d$ and $d = 10$ is the dimensionality. In line with ([Humbert et al. 2023](#)), the response variable is defined as

$$Y_i^k | X_i^k \stackrel{iid}{\sim} \text{Poisson}(\sin^2(\bar{X}_i^k) + 0.1) + 0.03\bar{X}_i^k \mathcal{N}(0, 1) + \mathbb{1}[\text{Uniform}([0, 1]) < 0.01] \mathcal{N}(0, 5),$$

where $\bar{X}_i^k = \sum_{l=1}^d [X_i^k]_l$. Data heterogeneity is simulated in the same way as for the synthetic Gaussian data.

Airfoil data ([Brooks et al. 1989](#)): This NASA dataset arose from studying different sizes of NACA 0012 airfoils under various conditions. It consists of 1503 instances of $d = 5$ covariates and 1 response. The covariates are frequency in Hertz, angle of attack in degrees, chord length in meters, free-stream velocity in meters per second, and suction side displacement thickness in meters. The covariates are normalized using the min-max rule. The response is the scaled sound pressure level in decibels. The frequency and suction side displacement thickness are log-transformed in our numerical experiments.

Data heterogeneity is simulated using *exponential tilting* as in [Tibshirani et al. \(2019\)](#). This is done as it allows the oracle baseline to know the true density ratio weights up to proportionality. For each data agent $k \in [K]$, data points are sampled with replacement with probabilities proportional to $\exp(X^\top \zeta^k)$ where $\zeta^k \in \mathbb{R}^d$ are tilting arrays. By construction, $[\text{d}\mathbb{P}/\text{d}\mathbb{P}^k](X) \propto \exp(X^\top (\zeta^1 - \zeta^k))$. We evaluate three setting with varying degrees of data heterogeneity. In the severe case, we generate $[\zeta^1]_l \stackrel{iid}{\sim} \text{Uniform}([1, 3]) \mathbb{1}[l \leq \lfloor d/4 \rfloor]$ for $l \in [d]$ and $[\zeta^k]_l \stackrel{iid}{\sim} \text{Uniform}([0, 2]) \mathbb{1}[l > \lfloor d/4 \rfloor]$ for $k \in \{2, \dots, K\}$ and $l \in [d]$. In the moderate case, we generate $[\zeta^1]_l \stackrel{iid}{\sim} \text{Uniform}([0.5, 1.5]) \mathbb{1}[l \leq$

$\lfloor d/4 \rfloor$ for $l \in [d]$ and $[\zeta^k]_l \stackrel{iid}{\sim} \text{Uniform}([0, 1])\mathbb{1}[l > \lfloor d/4 \rfloor]$ for $k \in \{2, \dots, K\}$ and $l \in [d]$. In the mild case, we generate $[\zeta^1]_l \stackrel{iid}{\sim} \text{Uniform}([0.25, 0.75])\mathbb{1}[l \leq \lfloor d/4 \rfloor]$ for $l \in [d]$ and $[\zeta^k]_l \stackrel{iid}{\sim} \text{Uniform}([0, 0.5])\mathbb{1}[l > \lfloor d/4 \rfloor]$ for $k \in \{2, \dots, K\}$ and $l \in [d]$. The severe case is the one studied in Section 3.

Bike data (Fanaee-T & Gama 2013): With this dataset we are predicting hourly bike sharing renting counts in Washington, D.C., and the data contains 17379 instances with $d = 9$ covariates and 1 response. The covariates are the hour of the day, whether it is a holiday (if it is a holiday it is 1, otherwise it is 0), the day of the week, whether it is a working day (if day is neither weekend nor holiday it is 1, otherwise it is 0), the weather (1 means clear sky or few clouds, 2 means cloudy, 3 means light precipitation, 4 means heavy precipitation), normalized temperature (Celsius divided by 41), normalized feeling temperature (Celsius divided by 50), relative humidity, and normalized wind speed (meters per second divided by 67). The covariates are normalized using the min-max rule. The response is the hourly bike sharing renting counts. Data heterogeneity is simulated in the same way as for the airfoil data.

Concrete data (Yeh 1998): This concrete compressive strength dataset consists of 1030 instances with $d = 8$ covariates and 1 response. The covariates are concentrations in kilograms per cubic meter of cement, blast furnace slag, fly ash, water, superplasticizer, coarse aggregate, fine aggregate, and age given in days. The covariates are normalized using the min-max rule. The response is the concrete compressive strength measured in megapascals. Data heterogeneity is simulated in the same way as for the airfoil data.

Crime data (Redmond 2009): This dataset concerns the prediction of violent crimes across communities in the US containing 1994 instances with $d = 41$ covariates and 1 response. The covariates cover aspects of demographic composition, socioeconomic status, labor market, and law enforcement presence. The covariates are normalized using the min-max rule. The response is the total number of violent crimes per 10^5 population. Data heterogeneity is simulated in the same way as for the airfoil data.

Star data (Achilles et al. 2008): This arose from studying how pupil-teacher ratios impact student performance in Tennessee. The dataset contains 3754 instances with $d = 20$ covariates and 1 response. The covariates cover aspects of student background and demographics, teacher characteristics, classroom and treatment assignment, and school-level attributes. The covariates are normalized using the min-max rule. The response is the achievement score. Data heterogeneity is simulated in the same way as for the airfoil data.

Protein data (Rana 2013): This dataset deals with physicochemical properties of protein tertiary structure and consists of 45730 instances with $d = 9$ covariates and 1 response. The covariates are the total surface area, the non-polar exposed area, the fractional area of exposed non-polar residue, the fractional area of exposed non-polar part of the residue, the molecular mass weighted exposed area, the average deviation from the standard exposed area of residue, the Euclidean distance, the secondary structure penalty, and the spatial distribution constraints. The response is the size of the residue. Data heterogeneity is simulated in the same way as for the airfoil data.

CIFAR-10 data (Hendrycks & Dietterich 2019): The CIFAR-10 data is a well-studied image classification dataset of 60000 total instances with labels airplane, automobile, bird, cat, deer, dog, frog, horse, ship, and truck with images in resolution $d = 32 \times 32 \times 3$. The CIFAR-10C dataset consists of the CIFAR-10 data contaminated with various types of noise of varying levels of severity (from 0-4). We restrict our attention to the brightness contamination, and evaluate three setting with varying degrees of data heterogeneity. In the severe case, we simulate data heterogeneity by sampling images random uniformly and contaminating the images with severity level $s \in \{0, 1, 2, 3, 4\}$ with probability proportional to $[\eta^k]_s \stackrel{iid}{\sim} \text{Uniform}([0, 1])$ for $k \in [K]$. In the moderate case, we simulate data heterogeneity by sampling images random uniformly and contaminating the images with severity level $s \in \{0, 1, 2\}$ with probability proportional to $[\eta^k]_s \stackrel{iid}{\sim} \text{Uniform}([0, 1])$ for $k \in [K]$. In the mild case, we simulate data heterogeneity by sampling images random uni-

formly and contaminating the images with severity level $s \in \{0, 1\}$ with probability proportional to $[\eta^k]_s \stackrel{iid}{\sim} \text{Uniform}([0, 1])$ for $k \in [K]$. The severe case is the one studied in Section 3.

S3.2 Details of benchmarks

CP: Standard CP calibrates using local scores $\hat{s}_1^1, \dots, \hat{s}_{n_1}^1$. To achieve MC at level α , the local quantile $Q_\alpha = \text{Quantile}(1 - \alpha; \frac{1}{n_1+1} (\sum_{i=1}^{n_1} \delta_{\hat{s}_i^1} + \delta_\infty))$ is computed and the prediction set is constructed as $\mathcal{C}_\alpha(X) = \{Y \in \mathcal{Y} : \hat{s}(X, Y) \leq Q_\alpha\}$. To achieve CCC given levels α and δ , α^* is determined as the largest α' such that $F_{\text{Beta}}(1 - \alpha; (1 - \alpha')(n_1 + 1), \alpha'(n_1 + 1)) \leq \delta$ where F_{Beta} is the CDF of the Beta distribution. The local quantile Q_{α^*} is then evaluated, and the prediction set is constructed as $\mathcal{C}_{\alpha^*}(X)$.

FGLCP (Min et al. 2025): This baseline corresponds to *PF2* of Min et al. (2025). First, the dataset \mathcal{D}^1 is split into two disjoint datasets $\mathcal{D}_{\text{eng}}^1$ and $\mathcal{D}_{\text{cal}}^1$, where $\mathcal{D}_{\text{eng}}^1$ will be used for the engression task and $\mathcal{D}_{\text{cal}}^1$ is used for the model calibration. The method then uses datasets $\mathcal{D}_{\text{eng}}^1$ and \mathcal{D}^k for $k \in \{2, \dots, K\}$ to approximate the conditional distribution $F(\hat{s}(X, Y)|X)$, yielding localized scores $\hat{s}_{\text{loc}}(X, Y) = \hat{F}(\hat{s}(X, Y)|X)$ for $(X, Y) \in \mathcal{D}_{\text{cal}}^1$. The conformal prediction set is then constructed as $\mathcal{C}_\alpha^{\text{glcp}} = \{Y \in \mathcal{Y} : \hat{s}_{\text{loc}}(X, Y) \leq Q_\alpha^{\text{glcp}}\}$ where

$$Q_\alpha^{\text{glcp}} = \text{Quantile}\left(1 - \alpha; \frac{1}{|\mathcal{D}_{\text{cal}}^1| + 1} \left(\sum_{(X, Y) \in \mathcal{D}_{\text{cal}}^1} \delta_{\hat{s}_{\text{loc}}(X, Y)} + \delta_1 \right)\right).$$

To compute $\hat{F}(\hat{s}(X, Y)|X)$, a federated engression algorithm is employed based on a fully connected neural network with two hidden layers each with 50 hidden units followed by Platt calibration. The engression data is randomly split in a 9:1 ratio for classifier training and Platt calibration. The reader is referred Min et al. (2025) for further details on the federated engression algorithm used to compute $\hat{F}(\hat{s}(X, Y)|X)$.

FCP: Standard FCP aggregates all the scores \hat{s}_i^k for $k \in [K]$ and $i \in [n_k]$. To achieve MC at level α , the quantile $Q_\alpha = \text{Quantile}(1 - \alpha; \frac{1}{\sum_{k=1}^K n_k + 1} (\sum_{k=1}^K \sum_{i=1}^{n_k} \delta_{\hat{s}_i^k} + \delta_\infty))$ is computed and the prediction set is constructed as $\mathcal{C}_\alpha(X) = \{Y \in \mathcal{Y} : \hat{s}(X, Y) \leq Q_\alpha\}$. To achieve CCC given levels α and δ , α^* is determined as the largest α' such that

$$F_{\text{Beta}}\left(1 - \alpha; (1 - \alpha') \left(\sum_{k=1}^K n_k + 1 \right), \alpha' \left(\sum_{k=1}^K n_k + 1 \right)\right) \leq \delta,$$

where F_{Beta} is the CDF of the Beta distribution. The local quantile Q_{α^*} is then evaluated, and the prediction set is constructed as $\mathcal{C}_{\alpha^*}(X)$.

FCP-QQ (Humbert et al. 2023, 2024): For MC guarantee at level α , the quantile-of-quantiles method finds quantiles $\bar{\beta}$ and $\bar{\tau}$ by solving

$$(\bar{\beta}, \bar{\tau}) = \arg \min_{(\beta, \tau) \in (0, 1)^2} \{ \mathbb{E}[U_\beta^{(\lceil K(1-\tau) \rceil)}] : \mathbb{E}[U_\beta^{(\lceil K(1-\tau) \rceil)}] \geq 1 - \alpha \},$$

where $U_\beta^k \sim \text{Beta}((1 - \beta)(n_k + 1), \beta(n_k + 1))$, and $U_\beta^{(t)}$ is the t -th smallest among $U_\beta^1, \dots, U_\beta^K$. This is solvable using that $U_\beta^{(\lceil K(1-\tau) \rceil)}$ follows a Beta-Beta distribution. Given the quantiles $\bar{\beta}$ and $\bar{\tau}$, the quantile-of-quantiles $Q_{\bar{\beta}, \bar{\tau}} = \text{Quantile}(1 - \bar{\tau}; \frac{1}{K} \sum_{k=1}^K \delta_{Q_{\bar{\beta}}^k})$ where $Q_{\bar{\beta}}^k = \text{Quantile}(1 - \bar{\beta}; \frac{1}{n_k+1} (\sum_{j=1}^{n_k} \delta_{\hat{s}_j^k} + \delta_\infty))$ is computed and the prediction set is constructed as $\mathcal{C}_{\bar{\beta}, \bar{\tau}}(X) = \{Y \in \mathcal{Y} : \hat{s}(X, Y) \leq Q_{\bar{\beta}, \bar{\tau}}\}$. Likewise, the CCC guarantee with levels α and δ can be satisfied by finding quantiles $\bar{\beta}_c$ and $\bar{\tau}_c$ minimizing the CCC while maintaining

$$\mathbb{P}_{\mathcal{D}}(\mathbb{P}(Y \in \mathcal{C}_{\bar{\beta}_c, \bar{\tau}_c}(X)|\mathcal{D}) \geq 1 - \alpha) \geq 1 - \delta.$$

This can practically be realized by exploiting that the left-hand side of the above inequality is equal to $\mathbb{P}(U_{\bar{\beta}_c}^{(\lceil K(1-\tau_c) \rceil)} \geq 1 - \alpha)$ and again using that $U_{\bar{\beta}_c}^{(\lceil K(1-\tau_c) \rceil)}$ follows a Beta-Beta distribution.

FWCP (Plassier et al. 2023, 2024): The federated weighted conformal prediction (FWCP) approach uses all the scores \hat{s}_i^k for $k \in [K]$ and $i \in [n_k]$ to determine the quantile of the score distribution weighted by an estimate, $\hat{\omega}'$, of $\omega'(X) = [\text{d}\mathbb{P}_X / \sum_{k=2}^K \text{d}\mathbb{P}_X^k / (K-1)](X)$. The density ratio is estimated by fitting a binary classifier to data $\{(\tilde{X}_i^1, 1)\}_{i=1}^{\tilde{n}_1} \cup (\bigcup_{k=2}^K \{(\tilde{X}_i^k, 0)\}_{i=1}^{\tilde{n}_k})$. As the binary classifier we employ a fully connected neural network with a single hidden layer using the standard implementation in `scikit-learn`. To achieve MC at level α , the quantile

$$Q_\alpha = \text{Quantile}\left(1 - \alpha : \frac{\sum_{k=1}^K \sum_{i=1}^{n_k} \hat{\omega}'(X_i^k) \delta_{\hat{s}_i^k} + \hat{\omega}'(X) \delta_\infty}{\sum_{k=1}^K \sum_{i=1}^{n_k} \hat{\omega}'(X_i^k) + \hat{\omega}'(X)}\right),$$

is computed and the prediction set is constructed as $\mathcal{C}_\alpha(X) = \{Y \in \mathcal{Y} : \hat{s}(X, Y) \leq Q_\alpha\}$. To achieve CCC given levels α and δ , α^* is determined as the largest α' such that

$$F_{\text{Beta}}\left(1 - \alpha; (1 - \alpha') \left(\sum_{k=1}^K n_k + 1\right), \alpha' \left(\sum_{k=1}^K n_k + 1\right)\right) \leq \delta,$$

where F_{Beta} is the CDF of the Beta distribution. The local quantile Q_{α^*} is then evaluated, and the prediction set is constructed as $\mathcal{C}_{\alpha^*}(X)$.

FWCP-QQ (ours): A variant of FWCP using a quantile-of-quantiles approach is also included as a benchmark. The quantiles $\bar{\beta}$ and $\bar{\tau}$ satisfying the MC condition are found as in the *FCP-QQ* approach. Given the quantiles $\bar{\beta}$ and $\bar{\tau}$, compute $Q_{\bar{\beta}, \bar{\tau}} = \text{Quantile}(1 - \bar{\tau} : \frac{1}{K} \sum_{k=1}^K \delta_{Q_{\bar{\beta}}^k})$ where $Q_{\bar{\beta}}^k$ is the weighted quantile

$$Q_{\bar{\beta}}^k = \text{Quantile}\left(1 - \bar{\beta} : \frac{\sum_{j=1}^{n_k} \hat{\omega}'_j \delta_{\hat{s}_j^k} + \hat{\omega}'(X) \delta_\infty}{\bar{\omega}' + \hat{\omega}'(X)}\right),$$

using the same weights as for *FWCP*. The prediction set is constructed as $\mathcal{C}_{\bar{\beta}, \bar{\tau}}(X) = \{Y \in \mathcal{Y} : \hat{s}(X, Y) \leq Q_{\bar{\beta}, \bar{\tau}}\}$. Likewise, the CCC guarantee with levels α and δ can be satisfied by finding quantiles $\bar{\beta}_c$ and $\bar{\tau}_c$ as in *FCP-QQ*.

PFWCP (ours): This is the core methodology presented in Section 2.

osPFWCP (ours): This is the communication efficient one-shot method detailed in Section 2.

osPFWGLCP (ours): This benchmark is a variant of the *osPFWCP* in which federated engression is used to localize the score function as in the *FGLCP* benchmark proposed by Min et al. (2025). Hence, this method combines the benefits of score function localization of Min et al. (2025) with the federation of calibration information with personalized statistical validity of this work. The baseline divides the datasets \mathcal{D}^k into two disjoint datasets $\mathcal{D}_{\text{eng}}^k$ and $\mathcal{D}_{\text{cal}}^k$ with a 1:1 ratio, where $\mathcal{D}_{\text{eng}}^k$ will be used for the engression task and $\mathcal{D}_{\text{cal}}^k$ is used for the model calibration. The method then uses datasets $\mathcal{D}_{\text{eng}}^k$ for $k \in [K]$ to approximate the conditional distribution $F(\hat{s}(X, Y)|X)$, yielding localized scores $\hat{s}_{\text{loc}}(X, Y) = \hat{F}(\hat{s}(X, Y)|X)$ for $(X, Y) \in \bigcup_{k=1}^K \mathcal{D}_{\text{cal}}^k$. The conformal prediction set is then constructed using the weighted-quantile-of-quantiles approach with one-shot communication as presented in Section 2, using \hat{s}_{loc} in place of \hat{s} . As in the *FGLCP* benchmark, $\hat{F}(\hat{s}(X, Y)|X)$ is computed using a federated engression algorithm based on a fully connected neural network with two hidden layers each with 50 hidden units followed by Platt calibration. The engression data is randomly split in a 9:1 ratio for classifier training and Platt calibration.

S3.3 Additional implementation details

Prediction model specifications and training: The prediction model is given by a fully connected neural network trained with federated learning on the training data of all the participating data agents. For the synthetic datasets, two hidden layers each with 30 hidden units is used. For the real regression datasets, three hidden layers are used with 500, 200, and 100 hidden units, respectively. For the *cifar10* data, three hidden layers are used with 200, 100, and 50 hidden units, respectively, acting on the principal components trained to explain at least 90 % of the variance.

For the regression tasks, the hidden layer activations are LeakyReLU, and the neural networks are trained using the adam algorithm with the mean squared error loss. The batch size is 32, the learning rate is 0.001, and the number of epochs is 5000.

For the classification task, the hidden layer activations are ReLU with softmax output activation, and the neural networks are trained using the adam algorithm with the cross entropy loss and an L_2 regularization term with parameter 0.0001. The batch size is 32, the learning rate is 0.001, and the number of epochs is 5000.

Density ratio estimation: For the synthetic datasets, the binary classifiers used to estimate the density ratios are specified as fully connected neural networks with a single 10-unit hidden layer employing ReLU hidden layer activations with sigmoid output activation. For the real regression datasets, we use a single 30-unit hidden layer. For the *cifar10* dataset, we use also a fully connected neural network with a single 10-unit hidden layer, here acting on the principal components trained to explain at least 90 % of the variance. The neural networks are trained using the adam algorithm with the cross entropy loss and an L_2 regularization term with parameter 0.0001. The batch size is set to 200, the learning rate is set to 0.001, and the number of epochs used is 600.

Hyperparameter selection: The choice of N_{rep} (see Procedure 1) represents an important trade-off between computational complexity and the error made in solving Eq. (3). The algorithm simulates data $U_{\beta,i}^{(\tau)} \simeq \mathbb{P}(Y \in \mathcal{C}_{\beta,\tau}^{\text{wqq}}(X)|\mathcal{D})$ and, for MC, uses the sample mean to approximate $\mathbb{P}(Y \in \mathcal{C}_{\beta,\tau}^{\text{wqq}}(X)) = \mathbb{E}[\mathbb{P}(Y \in \mathcal{C}_{\beta,\tau}^{\text{wqq}}(X)|\mathcal{D})]$. The variance of the sample mean equals $\text{Var}[U_{\beta,i}^{(\tau)}]/N_{\text{rep}}$. Since $U_{\beta,i}^{(\tau)}$ are random variables defined on $[0, 1]$, their variance is upper bounded by $1/4$, meaning that the standard deviation of the sample mean is upper bounded by $1/(2\sqrt{N_{\text{rep}}})$. Practically, it is desirable to have $1/(2\sqrt{N_{\text{rep}}}) \ll \alpha$, i.e., $N_{\text{rep}} \gg 1/(4\alpha^2)$. For CCC we are concerned with the variance of the empirical quantile estimator which has asymptotic expansion $\alpha(1-\alpha)/(N_{\text{rep}}f^2(F^{-1}(1-\alpha)))$ where F^{-1} and f are the quantile and density functions of $U_{\beta}^{(\tau)}$, respectively (Stuart & Ord 1994), leading to the guideline $N_{\text{rep}} \gg \alpha(1-\alpha)/(\delta^2 f^2(F^{-1}(1-\alpha)))$. Since f and F^{-1} are unknown prior to running the algorithm, this is not directly applicable but the expression is inverse proportional to δ^2 giving some intuition still. In the numerical experiments, we use $N_{\text{rep}} = 2000$ for MC guarantees, and $N_{\text{rep}} = 4000$ for CCC guarantees.

In Procedure 1, a search space $\mathcal{G} \subset (0, 1) \times [0, 1)$ on the quantiles (β, τ) must be provided. In this work, we design this as $\{\alpha, \alpha + \Delta_{\beta}, \dots, 1/4\} \times \{0, \Delta_{\tau}, \dots, 1/2\}$ where $\Delta_{\beta} = (1/4 - \alpha)/21$ and $\Delta_{\tau} = 1/42$ are the step sizes. This ensures that β^* is never small to the point of risking $Q_{\beta^*}^k$ being infinite, and generally, a value of β closer to $1/2$ provides more stable prediction sets. For the one-shot procedures, osPFWCP and osPFWGLCP, the search space is only on the τ quantile and is designed as $\{0, \Delta'_{\tau}, \dots, 1 - \max(w_1, \dots, w_K)\}$ where $\Delta'_{\tau} = (1 - \max(w_1, \dots, w_K))/50$, thereby ensuring that $1 - \tau^*$ is always greater than $\max(w_1, \dots, w_K)$ such that a valid quantile can be determined.

S3.4 Details to reproduce Figure 3

To illustrate the core principle motivated by Proposition 1, we conducted a numerical experiment on the Tennessee’s student teacher achievement ratio dataset (Achilles et al. 2008). With this data, we evaluated the CCC for CP with and without covariate shift, WCP with weights estimated using logistic regression, as well as CP without covariate shift using the estimated effective sample size. As in Tibshirani et al. (2019), we simulated a covariate shift through exponential tilting, specifically, the calibration data with covariate shift samples the dataset with replacement with probabilities proportional to $\exp(X^{\top}\zeta)$ where $\zeta = -[2.5, 1, 2, 1, 0.5, 1.5, 1, 1.5, 0.5, 0.5, 0, 0.5, 0.5, 0, 0, 0.5, 1.5, 2.5, 2, 0]^{\top}$. The elements of this tilting array were generated random uniformly from $\{0, -0.5, -1, \dots, -3\}$. The significance level was set to $\alpha = 0.1$, and the calibration dataset had $n = 100$ samples. The empirical CCC is evaluated for 1000 Monte Carlo simulations of the calibration data with 1000 test points for each. The result is shown in Figure 3.

S4 Additional numerical results

Here, we provide additional numerical results to supplement those presented in Section 3. This includes results with additional benchmarks, specifically, *FCP* and the proposed methods using oracle weights (when these are known). Further, we include results with the three different levels of heterogeneity described in Section S3.1. Tables 4 and 5 shows extended versions of the Tables 2 and 3, i.e., the severe heterogeneity experiments. Tables 6 and 7 show results for the case of moderate heterogeneity while Tables 8 and 9 show the results for the case of mild heterogeneity. Overall, the results indicate the efficacy of the proposed *PFWCP* method to efficiently provide the specified statistical guarantees. Meanwhile, the one-shot techniques *osPFWCP* and *osPFWGLCP* show promising performance to provide MC guarantees but on occasion struggles to provide the specified CCC guarantees, due to the lessened flexibility in the quantile specifications. Using *osPFWGLCP* tends to provide efficient conformal prediction sets with less miscoverage than *osPFWCP*. Comparatively, the *FWCP-QQ* benchmark tends to be overly conservative, which is also to be expected considering that it does not adjust for the increased variance in the coverage due to the data heterogeneity. The *FWCP* benchmark is competitive in terms of providing MC guarantees, but tends to fail dramatically in satisfying CCC guarantees. A similar remark applies to the *FCP* and *FCP-QQ* benchmarks, although these techniques tend to be overly liberal in terms of both MC and CCC guarantees in the case of severe heterogeneity.

Table 4: Severe heterogeneity. Marginal coverage (MC), conditional miscoverage (CMC), and efficiency (Eff.). Methods with MC above $1 - \alpha = 0.9$, above 0.89, and below 0.89 are marked by colors green, yellow, and red, respectively.

		gaussian	poisson	airfoil	protein	bike	concrete	crime	star	cifar10c
MC (%)	CP	89.57	89.77	89.49	89.48	89.42	89.65	89.58	89.65	89.16
	FGLCP	90.38	90.28	89.80	90.19	90.23	90.34	89.99	90.16	89.96
	FCP	90.49	89.84	86.44	90.09	88.19	84.26	89.00	88.70	89.06
	FCP-QQ	88.70	89.97	86.48	90.20	88.20	84.17	89.11	88.78	89.40
	FWCP	90.22	89.81	92.32	90.51	89.57	89.93	89.11	89.74	85.23
	FWCP-QQ	92.13	92.34	94.06	91.09	91.10	91.78	92.11	91.82	85.87
	PFWCP	92.01	91.26	91.73	90.67	90.31	90.78	90.47	90.43	90.32
	PFWCP (oracle)	93.68	92.81	91.73	90.63	92.42	91.87	91.75	90.89	N/A
	osPFWCP	89.07	90.06	90.12	90.28	88.16	89.42	89.00	89.68	88.39
	osPFWCP (oracle)	89.72	90.00	89.94	90.25	89.49	90.17	89.87	89.96	N/A
	osPFWGLCP	90.19	90.17	89.66	90.11	89.21	89.65	89.27	89.75	85.26
	osPFWGLCP (oracle)	90.22	89.91	89.72	90.28	89.78	90.00	89.70	89.94	N/A
	CMC (%)	CP	2.67	2.54	2.64	2.70	2.60	2.71	2.46	2.64
FGLCP		3.36	3.45	3.58	3.51	3.25	3.44	3.36	3.47	3.52
FCP		1.31	1.31	3.58	1.24	2.05	5.74	1.49	1.78	2.40
FCP-QQ		2.54	1.41	3.57	1.44	2.17	5.83	1.57	1.82	2.54
FWCP		2.37	1.66	2.51	1.32	2.04	1.58	2.94	1.76	6.52
FWCP-QQ		2.53	2.61	4.09	1.62	1.89	2.21	2.67	2.33	6.30
PFWCP		2.68	1.94	2.15	1.56	1.79	1.85	1.95	1.66	2.89
PFWCP (oracle)		3.82	3.10	2.30	1.56	2.87	2.35	2.32	1.82	N/A
osPFWCP		2.11	1.57	1.64	1.42	2.25	1.75	1.92	1.54	2.76
osPFWCP (oracle)		1.84	1.81	1.69	1.38	1.78	1.74	1.61	1.68	N/A
osPFWGLCP		2.11	1.75	1.82	1.53	1.84	2.16	2.10	1.82	5.14
osPFWGLCP (oracle)		2.12	2.11	1.85	1.54	1.88	2.13	2.00	1.90	N/A
Eff.		CP	0.09	9.84	6.52	2.25	2.04	20.75	2.12	38.61
	FGLCP	0.09	15.96	6.73	2.36	2.45	23.14	2.29	40.10	9.00
	FCP	0.09	9.68	5.47	2.27	1.91	15.18	2.05	36.60	8.93
	FCP-QQ	0.09	9.75	5.47	2.28	1.92	15.11	2.06	36.77	8.96
	FWCP	0.09	9.71	7.49	2.31	2.03	20.72	2.15	38.27	8.55
	FWCP-QQ	0.10	12.20	8.35	2.36	2.31	22.76	2.49	43.39	8.61
	PFWCP	0.10	10.58	7.05	2.33	2.16	21.37	2.26	39.60	9.05
	PFWCP (oracle)	0.10	15.40	7.14	2.33	2.53	22.52	2.41	41.18	N/A
	osPFWCP	0.09	9.80	6.45	2.29	1.92	19.66	2.07	38.11	8.86
	osPFWCP (oracle)	0.09	9.83	6.39	2.29	2.03	20.47	2.13	38.77	N/A
	osPFWGLCP	0.08	9.70	6.22	2.22	2.06	18.88	2.02	37.29	8.53
	osPFWGLCP (oracle)	0.08	10.24	6.22	2.24	2.15	19.22	2.06	38.05	N/A

Table 5: Severe heterogeneity. Calibration-conditional coverage (CCC), conditional miscoverage (CMC), and efficiency (Eff.). Methods with CCC above $1 - \delta = 0.9$, above 0.8, and below 0.8 are marked by colors green, yellow, and red, respectively.

		gaussian	poisson	airfoil	protein	bike	concrete	crime	star	cifar10c
CCC (%)	CP	86.60	87.20	86.00	86.80	84.80	86.40	84.80	86.80	86.80
	FGLCP	90.40	93.00	91.20	90.80	90.40	91.00	89.40	90.60	91.80
	FCP	100.00	82.80	29.40	80.60	33.00	3.20	75.00	60.20	71.00
	FCP-QQ	100.00	85.60	42.20	84.00	42.40	7.60	80.40	67.40	62.40
	FWCP	79.40	89.40	97.80	89.20	77.40	74.60	96.80	83.00	65.60
	FWCP-QQ	97.80	98.80	99.60	95.00	95.80	96.40	96.00	97.00	61.40
	PFWCP	99.20	96.60	97.00	92.80	91.60	91.00	85.60	92.80	88.40
	PFWCP (oracle)	99.40	99.80	98.40	92.20	99.00	96.60	97.20	97.60	N/A
	osPFWCP	93.20	90.40	88.20	87.80	63.60	77.20	69.20	81.40	77.40
	osPFWCP (oracle)	88.40	90.60	88.80	85.00	90.00	88.40	83.20	90.20	N/A
	osPFWGLCP	95.00	95.60	88.00	91.80	87.40	88.40	86.20	94.80	87.80
	osPFWGLCP (oracle)	94.60	96.20	86.20	93.40	91.60	92.60	91.20	94.20	N/A
CMC (%)	CP	3.37	3.61	3.28	3.66	3.39	3.40	3.42	3.52	3.42
	FGLCP	5.02	5.16	4.85	5.11	4.70	5.04	4.92	4.94	5.05
	FCP	5.11	1.62	1.70	1.54	1.51	3.87	1.44	1.39	2.29
	FCP-QQ	5.89	1.99	1.60	1.80	1.41	3.37	1.68	1.62	2.28
	FWCP	2.31	2.85	4.34	1.82	2.47	1.78	6.26	2.14	4.49
	FWCP-QQ	4.29	5.05	6.32	2.63	3.68	3.58	5.97	3.64	4.54
	PFWCP	4.99	3.70	3.74	2.42	2.83	2.79	3.00	2.65	4.04
	PFWCP (oracle)	5.42	5.22	4.14	2.37	4.77	3.86	4.00	3.38	N/A
	osPFWCP	2.93	2.58	2.41	2.05	1.74	1.94	1.94	2.07	2.60
	osPFWCP (oracle)	2.52	2.90	2.41	1.99	2.75	2.51	2.46	2.43	N/A
	osPFWGLCP	4.09	3.46	2.63	2.57	2.43	2.97	2.57	2.99	5.06
	osPFWGLCP (oracle)	4.09	4.00	2.72	2.73	3.22	3.50	2.88	3.07	N/A
Eff.	CP	0.05	10.75	7.21	2.64	2.38	25.99	2.53	43.90	9.28
	FGLCP	0.06	22.93	9.00	2.97	3.50	35.70	3.07	47.68	9.46
	FCP	0.05	9.51	5.82	2.42	1.91	16.30	2.17	39.43	9.10
	FCP-QQ	0.05	9.72	5.94	2.45	1.96	16.81	2.22	40.15	9.05
	FWCP	0.04	10.24	7.86	2.46	2.21	21.92	3.77	41.72	9.16
	FWCP-QQ	0.05	14.61	9.39	2.55	2.64	26.08	3.78	46.32	9.11
	PFWCP	0.05	11.16	7.33	2.53	2.39	24.34	2.66	43.05	9.36
	PFWCP (oracle)	0.06	18.14	7.63	2.52	2.86	26.60	2.85	45.32	N/A
	osPFWCP	0.05	10.06	6.70	2.48	2.08	22.11	2.28	41.40	9.17
	osPFWCP (oracle)	0.05	10.61	6.71	2.47	2.38	23.46	2.41	42.34	N/A
	osPFWGLCP	0.06	11.34	7.12	2.50	2.42	25.06	2.39	41.80	9.44
	osPFWGLCP (oracle)	0.07	15.60	7.16	2.51	2.76	26.86	2.51	42.88	N/A

Table 6: Moderate heterogeneity. Marginal coverage (MC), conditional miscoverage (CMC), and efficiency (Eff.). Methods with MC above $1 - \alpha = 0.9$, above 0.89, and below 0.89 are marked by colors green, yellow, and red, respectively.

		gaussian	poisson	airfoil	protein	bike	concrete	crime	star	cifar10c
MC (%)	CP	89.74	89.93	89.51	89.87	89.73	89.71	89.74	89.70	89.25
	FGLCP	90.46	90.31	90.05	90.30	90.57	90.39	90.27	90.60	90.18
	FCP	88.97	90.11	89.86	90.06	89.47	89.17	90.17	89.45	89.46
	FCP-QQ	89.08	90.20	89.99	90.23	89.57	89.28	90.34	89.58	89.96
	FWCP	90.93	90.72	91.02	89.97	90.39	90.53	91.66	90.08	86.33
	FWCP-QQ	91.37	91.74	91.79	90.58	91.39	91.42	92.47	90.69	86.51
	PFWCP	91.00	90.73	90.74	90.40	91.01	90.60	91.72	90.29	90.58
	PFWCP (oracle)	91.00	90.91	90.70	90.71	90.98	90.60	90.73	90.68	N/A
	osPFWCP	89.61	89.92	90.08	90.11	90.02	89.77	90.06	89.72	89.18
	osPFWCP (oracle)	90.10	90.07	90.08	90.52	90.03	89.99	89.85	90.11	N/A
	osPFWGLCP	88.99	89.90	89.64	90.22	89.63	89.40	89.12	90.01	88.37
	osPFWGLCP (oracle)	90.07	89.97	89.94	90.64	89.98	89.91	90.06	90.40	N/A
CMC (%)	CP	2.43	2.41	2.71	2.47	2.84	2.60	2.52	2.52	2.77
	FGLCP	3.44	3.50	3.44	3.46	3.46	3.39	3.48	3.40	3.46
	FCP	1.55	1.29	1.32	1.31	1.32	1.40	1.32	1.35	2.34
	FCP-QQ	1.61	1.44	1.52	1.38	1.42	1.40	1.51	1.48	2.52
	FWCP	2.32	1.54	1.63	1.33	1.37	1.52	2.16	1.29	6.03
	FWCP-QQ	2.23	2.09	2.10	1.44	1.85	1.99	2.70	1.56	6.04
	PFWCP	1.83	1.63	1.66	1.52	1.72	1.67	2.30	1.52	2.96
	PFWCP (oracle)	1.66	1.71	1.56	1.50	1.76	1.51	1.66	1.59	N/A
	osPFWCP	1.66	1.49	1.46	1.38	1.42	1.49	1.69	1.41	2.47
	osPFWCP (oracle)	1.37	1.46	1.43	1.42	1.42	1.39	1.52	1.38	N/A
	osPFWGLCP	2.03	1.63	1.73	1.55	1.70	1.75	1.97	1.61	3.11
	osPFWGLCP (oracle)	1.64	1.67	1.66	1.59	1.71	1.59	1.66	1.67	N/A
Eff.	CP	0.17	8.71	5.33	2.19	1.88	13.45	2.38	42.10	8.93
	FGLCP	0.20	15.36	6.38	2.28	2.10	18.36	2.43	47.40	9.02
	FCP	0.16	8.67	5.36	2.19	1.82	12.36	2.40	41.40	8.95
	FCP-QQ	0.16	8.71	5.40	2.20	1.83	12.51	2.41	41.56	9.00
	FWCP	0.18	8.88	5.70	2.18	1.89	13.81	2.57	42.27	8.64
	FWCP-QQ	0.18	9.28	5.95	2.23	1.96	15.07	2.71	43.15	8.65
	PFWCP	0.18	8.91	5.61	2.22	1.94	14.11	2.57	42.59	9.06
	PFWCP (oracle)	0.18	8.99	5.59	2.24	1.93	14.03	2.45	43.11	N/A
	osPFWCP	0.17	8.61	5.40	2.19	1.86	13.20	2.39	41.78	8.92
	osPFWCP (oracle)	0.17	8.66	5.40	2.22	1.86	13.37	2.37	42.27	N/A
	osPFWGLCP	0.16	8.72	5.39	2.18	1.79	13.21	2.17	42.58	8.84
	osPFWGLCP (oracle)	0.16	8.83	5.45	2.21	1.82	13.58	2.24	43.00	N/A

Table 7: Moderate heterogeneity. Calibration-conditional coverage (CCC), conditional miscoverage (CMC), and efficiency (Eff.). Methods with CCC above $1 - \delta = 0.9$, above 0.8, and below 0.8 are marked by colors green, yellow, and red, respectively.

		gaussian	poisson	airfoil	protein	bike	concrete	crime	star	cifar10c
CCC (%)	CP	87.60	84.20	85.00	84.20	86.40	84.60	87.00	83.40	84.80
	FGLCP	89.20	88.80	91.80	89.00	89.80	89.40	92.40	88.20	89.60
	FCP	74.40	88.40	77.80	76.80	60.00	64.20	80.60	71.00	59.60
	FCP-QQ	80.40	89.40	81.60	80.20	67.60	72.00	84.60	75.80	48.80
	FWCP	59.00	90.20	88.40	75.60	80.60	87.00	95.60	74.00	41.20
	FWCP-QQ	76.20	97.60	96.80	86.80	93.80	94.80	97.80	87.20	37.80
	PFWCP	94.20	93.00	90.60	84.60	92.20	94.00	95.00	84.40	86.80
	PFWCP (oracle)	92.80	93.20	90.00	88.60	93.40	90.40	91.80	89.60	N/A
	osPFWCP	79.40	88.00	84.00	80.60	79.80	83.60	89.20	77.60	72.20
	osPFWCP (oracle)	85.60	84.00	83.80	86.00	85.40	86.00	86.60	86.20	N/A
	osPFWGLCP	81.60	84.00	86.60	93.00	84.80	88.40	88.20	88.40	63.40
	osPFWGLCP (oracle)	89.60	88.60	88.60	94.40	87.80	91.40	91.80	90.40	N/A
CMC (%)	CP	3.39	3.46	3.45	3.42	3.46	3.44	3.47	3.55	3.14
	FGLCP	4.69	4.86	4.94	4.96	4.94	5.04	5.10	5.22	4.94
	FCP	1.41	1.90	1.60	1.58	1.33	1.37	1.70	1.42	2.39
	FCP-QQ	1.77	2.24	1.93	1.85	1.52	1.55	1.99	1.65	2.50
	FWCP	1.73	2.13	2.07	1.56	1.73	2.09	3.83	1.49	3.88
	FWCP-QQ	2.45	3.40	3.10	2.18	2.87	3.39	4.94	2.19	4.16
	PFWCP	3.00	2.75	2.50	2.15	2.75	2.66	3.80	2.13	4.01
	PFWCP (oracle)	2.67	2.66	2.51	2.21	2.90	2.60	2.76	2.54	N/A
	osPFWCP	1.96	2.12	1.93	1.91	1.90	2.00	2.46	1.77	2.51
	osPFWCP (oracle)	1.97	2.02	2.01	2.06	2.10	2.02	2.04	2.07	N/A
	osPFWGLCP	2.23	2.42	2.50	2.66	2.50	2.53	2.70	2.53	3.59
	osPFWGLCP (oracle)	2.63	2.76	2.66	2.87	2.81	2.73	2.69	2.69	N/A
Eff.	CP	0.05	8.76	6.89	2.48	2.16	16.65	2.67	44.36	9.26
	FGLCP	0.08	17.82	9.16	2.85	3.11	25.09	3.41	54.53	9.45
	FCP	0.04	8.14	6.01	2.29	1.88	13.52	2.39	39.97	9.06
	FCP-QQ	0.04	8.28	6.16	2.33	1.91	13.99	2.43	40.47	8.98
	FWCP	0.04	8.23	6.29	2.29	1.96	14.96	2.77	40.15	8.89
	FWCP-QQ	0.05	8.87	6.81	2.38	2.10	16.94	3.04	41.90	8.82
	PFWCP	0.05	8.51	6.49	2.37	2.08	15.83	2.79	41.59	9.36
	PFWCP (oracle)	0.05	8.57	6.47	2.38	2.10	15.71	2.57	42.31	N/A
	osPFWCP	0.04	8.24	6.18	2.34	1.97	14.77	2.52	40.75	9.15
	osPFWCP (oracle)	0.04	8.18	6.20	2.36	2.00	14.86	2.45	41.29	N/A
	osPFWGLCP	0.05	8.36	6.29	2.42	2.05	15.55	2.47	42.80	9.14
	osPFWGLCP (oracle)	0.05	8.85	6.35	2.45	2.15	15.80	2.45	43.49	N/A

Table 8: Mild heterogeneity. Marginal coverage (MC), conditional miscoverage (CMC), and efficiency (Eff.). Methods with MC above $1 - \alpha = 0.9$, above 0.89, and below 0.89 are marked by colors green, yellow, and red, respectively.

		gaussian	poisson	airfoil	protein	bike	concrete	crime	star	cifar10
MC (%)	CP	89.49	89.59	89.62	89.53	89.55	89.60	89.48	89.60	88.81
	FGLCP	90.30	90.25	90.01	90.09	90.19	90.21	90.03	90.20	90.39
	FCP	89.92	90.37	90.15	90.05	89.38	89.46	90.23	90.07	89.56
	FCP-QQ	90.03	90.40	90.31	90.13	89.49	89.67	90.39	90.26	90.06
	FWCP	88.68	89.98	89.90	90.07	90.79	89.83	91.00	89.72	86.81
	FWCP-QQ	89.84	90.63	90.52	90.61	91.48	90.49	91.73	90.32	87.02
	PFWCP	90.76	91.04	89.99	90.69	91.15	91.09	91.12	90.68	90.47
	PFWCP (oracle)	90.54	90.57	90.41	90.75	90.68	90.66	90.54	90.71	N/A
	osPFWCP	89.83	90.18	89.66	90.33	90.28	90.47	90.47	90.20	88.83
	osPFWCP (oracle)	90.09	90.11	90.18	90.52	90.09	90.41	90.20	90.52	N/A
	osPFWGLCP	89.22	89.78	89.81	90.36	90.19	90.15	89.73	90.12	86.90
	osPFWGLCP (oracle)	90.08	90.38	90.41	90.71	90.53	90.32	90.14	90.65	N/A
CMC (%)	CP	2.75	2.59	2.43	2.66	2.80	2.54	2.80	2.48	2.78
	FGLCP	3.44	3.38	3.40	3.38	3.63	3.63	3.66	3.46	3.54
	FCP	1.26	1.34	1.30	1.27	1.38	1.24	1.34	1.27	2.27
	FCP-QQ	1.39	1.52	1.46	1.43	1.46	1.33	1.47	1.43	2.53
	FWCP	2.01	1.35	1.31	1.27	1.41	1.22	1.58	1.30	4.77
	FWCP-QQ	1.83	1.58	1.42	1.43	1.84	1.33	2.02	1.39	4.70
	PFWCP	1.69	1.81	1.52	1.56	1.77	1.71	1.82	1.52	2.73
	PFWCP (oracle)	1.52	1.64	1.54	1.44	1.69	1.60	1.67	1.53	N/A
	osPFWCP	1.53	1.50	1.41	1.41	1.43	1.41	1.51	1.39	2.42
	osPFWCP (oracle)	1.36	1.47	1.32	1.39	1.38	1.34	1.42	1.38	N/A
	osPFWGLCP	1.98	1.63	1.56	1.66	1.63	1.69	1.71	1.52	3.46
	osPFWGLCP (oracle)	1.64	1.56	1.52	1.67	1.63	1.56	1.60	1.59	N/A
Eff.	CP	0.07	8.31	5.56	2.27	2.01	13.04	2.24	39.95	8.90
	FGLCP	0.09	14.94	6.31	2.35	2.25	16.24	2.44	43.59	9.04
	FCP	0.07	8.41	5.62	2.29	1.97	12.55	2.27	40.24	8.97
	FCP-QQ	0.07	8.44	5.66	2.30	1.98	12.83	2.28	40.50	9.02
	FWCP	0.07	8.28	5.55	2.29	2.09	12.95	2.33	39.74	8.70
	FWCP-QQ	0.07	8.53	5.73	2.33	2.15	13.79	2.40	40.66	8.72
	PFWCP	0.08	8.69	5.59	2.34	2.13	14.40	2.35	41.21	9.06
	PFWCP (oracle)	0.08	8.51	5.71	2.35	2.09	13.93	2.30	41.19	N/A
	osPFWCP	0.07	8.36	5.50	2.31	2.04	13.70	2.29	40.47	8.90
	osPFWCP (oracle)	0.07	8.35	5.63	2.33	2.03	13.63	2.26	40.88	N/A
	osPFWGLCP	0.07	8.34	5.51	2.30	2.00	12.84	2.17	40.28	8.70
	osPFWGLCP (oracle)	0.07	8.51	5.66	2.33	2.02	12.95	2.21	41.04	N/A

Table 9: Mild heterogeneity. Calibration-conditional coverage (CCC), conditional miscoverage (CMC), and efficiency (Eff.). Methods with CCC above $1 - \delta = 0.9$, above 0.8, and below 0.8 are marked by colors green, yellow, and red, respectively.

		gaussian	poisson	airfoil	protein	bike	concrete	crime	star	cifar10
CCC (%)	CP	89.20	87.20	83.00	84.40	86.40	85.40	88.40	84.60	84.40
	FGLCP	91.20	91.60	90.60	88.20	89.60	91.00	91.60	90.20	89.00
	FCP	78.20	85.40	83.20	77.80	72.60	71.60	85.80	82.00	63.60
	FCP-QQ	83.20	86.60	85.00	82.80	77.60	75.80	88.40	86.80	46.40
	FWCP	81.00	92.80	85.60	76.20	92.40	75.00	93.40	71.00	46.80
	FWCP-QQ	90.60	97.40	92.80	87.40	97.00	84.80	97.20	85.40	39.40
	PFWCP	95.80	97.20	86.80	90.00	93.80	94.00	91.40	90.00	79.80
	PFWCP (oracle)	90.60	91.40	90.80	90.80	90.00	90.00	92.20	90.20	N/A
	osPFWCP	87.20	89.20	82.00	87.60	90.00	88.40	86.80	87.00	65.40
	osPFWCP (oracle)	87.00	86.80	86.40	89.60	85.00	84.00	85.00	87.20	N/A
	osPFWGLCP	83.80	91.20	93.00	94.80	91.60	92.80	89.00	92.80	82.60
	osPFWGLCP (oracle)	90.60	93.80	94.60	95.80	91.40	91.80	91.40	94.40	N/A
CMC (%)	CP	3.49	3.46	3.48	3.52	3.31	3.48	3.65	3.57	3.29
	FGLCP	4.86	4.99	4.94	4.74	4.80	4.93	5.06	5.04	5.16
	FCP	1.55	1.68	1.73	1.57	1.44	1.38	1.79	1.63	2.28
	FCP-QQ	1.82	2.03	2.02	1.84	1.69	1.62	2.08	1.96	2.44
	FWCP	1.97	2.15	1.85	1.52	2.11	1.51	2.48	1.42	4.48
	FWCP-QQ	3.05	3.13	2.65	2.20	3.15	2.13	3.55	1.99	5.04
	PFWCP	3.04	3.11	2.11	2.40	2.72	2.67	2.69	2.28	3.25
	PFWCP (oracle)	2.41	2.36	2.41	2.29	2.37	2.38	2.50	2.36	N/A
	osPFWCP	2.12	2.27	1.74	2.06	2.09	2.26	2.14	1.99	2.39
	osPFWCP (oracle)	2.01	1.97	1.98	2.14	1.88	1.96	2.00	2.00	N/A
	osPFWGLCP	2.27	2.71	2.51	2.74	2.56	2.87	2.38	2.44	5.21
	osPFWGLCP (oracle)	2.54	2.72	2.81	2.88	2.70	2.75	2.57	2.71	N/A
Eff.	CP	0.05	11.58	6.09	2.65	2.28	16.67	2.56	46.88	9.29
	FGLCP	0.08	23.78	9.04	3.01	2.81	21.94	3.16	53.83	9.46
	FCP	0.05	10.14	5.24	2.43	2.05	13.62	2.28	42.81	9.08
	FCP-QQ	0.05	10.34	5.37	2.46	2.09	13.99	2.32	43.62	8.97
	FWCP	0.05	10.47	5.30	2.42	2.16	13.87	2.37	41.88	8.97
	FWCP-QQ	0.05	11.24	5.71	2.51	2.28	14.94	2.56	43.72	8.84
	PFWCP	0.05	11.24	5.41	2.54	2.23	15.68	2.41	44.37	9.27
	PFWCP (oracle)	0.05	10.62	5.58	2.53	2.19	15.33	2.38	44.52	N/A
	osPFWCP	0.05	10.54	5.23	2.50	2.15	15.04	2.32	43.63	9.10
	osPFWCP (oracle)	0.05	10.30	5.37	2.51	2.13	14.65	2.30	43.77	N/A
	osPFWGLCP	0.05	10.52	5.61	2.56	2.11	14.75	2.34	45.28	9.39
	osPFWGLCP (oracle)	0.05	10.58	5.77	2.58	2.12	14.51	2.37	45.76	N/A

S5 Use of Large Language Models

Large language models have been used for the purpose of text editing.

References

- Achilles, C., Bain, H. P., Bellott, F., Boyd-Zaharias, J., Finn, J., Folger, J., Johnston, J. & Word, E. (2008), ‘Tennessee’s student teacher achievement ratio (star) project’, Harvard Dataverse.
- Blanchard, G., Lee, G. & Scott, C. (2010), ‘Semi-supervised novelty detection’, *Journal of Machine Learning Research* **11**(99), 2973–3009.
- Brooks, T., Pope, D. & Marcolini, M. (1989), ‘Airfoil Self-Noise’, UCI Machine Learning Repository.
- Campagner, A., Biganzoli, E. M., Balsano, C., Cereda, C. & Cabitza, F. (2025), ‘Modeling unknowns: A vision for uncertainty-aware machine learning in healthcare’, *International Journal of Medical Informatics* **203**, 106014.
- Cherubin, G. (2019), ‘Majority vote ensembles of conformal predictors’, *Machine Learning* **108**(3), 475 – 488.
- Choi, K., Meng, C., Song, Y. & Ermon, S. (2022), Density ratio estimation via infinitesimal classification, in ‘proceedings of the 25th International Conference on Artificial Intelligence and Statistics’, Vol. 151 of *Proceedings of Machine Learning Research*, PMLR, pp. 2552–2573.
- Fanae-T, H. & Gama, J. (2013), ‘Event labeling combining ensemble detectors and background knowledge’, *Progress in Artificial Intelligence* **2**.
- Gretton, A., Smola, A., Huang, J., Schmittfull, M., Borgwardt, K. & Schölkopf, B. (2009), *Dataset Shift in Machine Learning*, Neural Information Processing Series, MIT Press, chapter 8.
- Hendrycks, D. & Dietterich, T. (2019), Benchmarking neural network robustness to common corruptions and perturbations, in ‘proceedings of the 7th International Conference on Learning Representations’, Curran Associates, Inc.
- Huang, J., Gretton, A., Borgwardt, K., Schölkopf, B. & Smola, A. (2006), Correcting sample selection bias by unlabeled data, in B. Schölkopf, J. Platt & T. Hoffman, eds, ‘Advances in Neural Information Processing Systems’, Vol. 19, MIT Press.
- Humbert, P., Le Bars, B., Bellet, A. & Arlot, S. (2023), One-shot federated conformal prediction, in ‘proceedings of the 40th International Conference on Machine Learning’, Vol. 202 of *Proceedings of Machine Learning Research*, PMLR, pp. 14153–14177.
- Humbert, P., Le Bars, B., Bellet, A. & Arlot, S. (2024), ‘Marginal and training-conditional guarantees in one-shot federated conformal prediction’.
URL: <https://arxiv.org/abs/2405.12567>
- Li, G., Zhang, Y., Wang, Y. & Wang, C. (2026), ‘Fcp-pro: Federated conformal prediction algorithm based on prototype similarity’, *Pattern Recognition* **172**, 112514.
- Lu, C., Yu, Y., Karimireddy, S. P., Jordan, M. I. & Raskar, R. (2023), Federated conformal predictors for distributed uncertainty quantification, in ‘proceedings of the 40th International Conference on Machine Learning’, Vol. 202 of *Proceedings of Machine Learning Research*, PMLR.
- McDiarmid, C. (1989), *On the method of bounded differences*, London Mathematical Society Lecture Note Series, Cambridge University Press, p. 148–188.
- Min, Y., Zhang, C., Peng, L. & Zou, C. (2025), Personalized federated conformal prediction with localization, in ‘proceedings of the 39th Annual Conference on Neural Information Processing Systems’.
- Nguyen, X., Wainwright, M. J. & Jordan, M. (2007), Estimating divergence functionals and the likelihood ratio by penalized convex risk minimization, in ‘proceedings of the 21st Annual Conference on Neural Information Processing Systems’, Vol. 20, Curran Associates, Inc.
- Perini, L., Bürkner, P.-C. & Klami, A. (2023), Estimating the contamination factor’s distribution in unsupervised anomaly detection, in ‘proceedings of the 40th International Conference on Machine Learning’, Vol. 202 of *Proceedings of Machine Learning Research*, PMLR, pp. 27668–27679.

- Plassier, V., Kotelevskii, N., Rubashevskii, A., Noskov, F., Velikanov, M., Fishkov, A., Horvath, S., Takac, M., Moulines, E. & Panov, M. (2024), Efficient conformal prediction under data heterogeneity, in ‘proceedings of the 27th International Conference on Artificial Intelligence and Statistics’, Vol. 238 of *Proceedings of Machine Learning Research*, PMLR, pp. 4879–4887.
- Plassier, V., Makni, M., Rubashevskii, A., Moulines, E. & Panov, M. (2023), Conformal prediction for federated uncertainty quantification under label shift, in ‘proceedings of the 40th International Conference on Machine Learning’, Vol. 202 of *Proceedings of Machine Learning Research*, PMLR, pp. 27907–27947.
- Pournaderi, M. & Xiang, Y. (2026), ‘Training-conditional coverage bounds under covariate shift’, *Transactions on Machine Learning Research*.
- Rana, P. (2013), ‘Physicochemical properties of protein tertiary structure’, UCI Machine Learning Repository.
- Redmond, M. (2009), ‘Communities and crime unnormalized’, UCI Machine Learning Repository.
- Rieke, N., Hancox, J., Li, W., Milletari, F., Roth, H. R., Albarqouni, S., Bakas, S., Galtier, M. N., Landman, B. A., Maier-Hein, K., Ourselin, S., Sheller, M., Summers, R. M., Trask, A., Xu, D., Baust, M. & Cardoso, M. J. (2020), ‘The future of digital health with federated learning’, *npj Digital Medicine* 3(1).
- Srinivasan, A., Vadlamani, A. T., Meghrazi, A. & Parthasarathy, S. (2025), ‘FedCF: Fair federated conformal prediction’.
URL: <https://arxiv.org/abs/2509.22907>
- Stuart, A. & Ord, K. J. (1994), *Kendall’s Advanced Theory of Statistics*, 6 edn, Edward Arnold, New York.
- Sugiyama, M., Krauledat, M. & Müller, K.-R. (2007), ‘Covariate shift adaptation by importance weighted cross validation’, *Journal of Machine Learning Research* 8(35), 985–1005.
- Sugiyama, M., Suzuki, T. & Kanamori, T. (2012), *Density Ratio Estimation in Machine Learning*, Cambridge University Press.
- Sugiyama, M., Suzuki, T., Nakajima, S., Kashima, H., von Büna, P. & Kawanabe, M. (2008), ‘Direct importance estimation for covariate shift adaptation’, *Annals of the Institute of Statistical Mathematics* 60(4), 699–746.
- Tibshirani, R. J., Foygel Barber, R., Candès, E. & Ramdas, A. (2019), Conformal prediction under covariate shift, in ‘proceedings of the 32nd Annual Conference on Neural Information Processing Systems’, Vol. 32, Curran Associates, Inc.
- Vejling, M. V., Biscio, C. A. N., Pandey, S. R. & Popovski, P. (2026), ‘Conformal data contamination tests for in-distribution data acquisition’.
URL: <https://openreview.net/forum?id=ABA4KBVzIw>
- Vovk, V., Gammerman, A. & Shafer, G. (2005), *Algorithmic Learning in a Random World*, Springer-Verlag, Berlin, Heidelberg.
- Wen, H., Simeone, O. & Xing, H. (2026), ‘Efficient federated conformal prediction with group-conditional guarantees’.
URL: <https://arxiv.org/abs/2603.14198>
- Yamada, M., Suzuki, T., Kanamori, T., Hachiya, H. & Sugiyama, M. (2011), Relative density-ratio estimation for robust distribution comparison, in ‘proceedings of the 25th Annual Conference on Neural Information Processing Systems’, Vol. 24, Curran Associates, Inc.
- Yeh, I.-C. (1998), ‘Modeling of strength of high-performance concrete using artificial neural networks’, *Cement and Concrete Research* 28(12), 1797–1808.
- Yu, H., Klami, A., Hyvarinen, A., Korba, A. & Chehab, O. (2025), Density ratio estimation with conditional probability paths, in ‘proceedings of the 42nd International Conference on Machine Learning’, Vol. 267 of *Proceedings of Machine Learning Research*, PMLR.